Journal Pre-proof

Multi O- and S-isotopes as tracers of black crusts formation under volcanic and non-volcanic atmospheric conditions in Sicily (Italy)

A. Aroskay, E. Martin, S. Bekki, G. Montana, L. Randazzo, P. Cartigny, A. Chabas, A. Verney-Carron

PII: S0048-9697(20)35812-5

DOI: https://doi.org/10.1016/j.scitotenv.2020.142283

Reference: STOTEN 142283

To appear in: *Science of the Total Environment*

Received date: 12 June 2020

Revised date: 4 September 2020

Accepted date: 7 September 2020

Please cite this article as: A. Aroskay, E. Martin, S. Bekki, et al., Multi O- and S-isotopes as tracers of black crusts formation under volcanic and non-volcanic atmospheric conditions in Sicily (Italy), *Science of the Total Environment* (2020), https://doi.org/10.1016/j.scitotenv.2020.142283

Multi O- and S-isotopes as tracers of black crusts formation under volcanic and non-volcanic atmospheric conditions in Sicily (Italy)

A.Aroskay [(1)*], E.Martin [(1)], S.Bekki [(2)], G.Montana [(3)], L.Randazzo [(4)], P.Cartigny [(5)], A.Chabas[(6)], A.Verney-Carron[(6)]

(1) Institut des Sciences de la Terre de Paris (ISTeP), Sorbonne Université, Paris, France
(2) Laboratoire Atmosphères, Milieux, Observations Spatiales (LATMOS), Sorbonne Université, Paris, France
(3) Dipartimento di Scienze della Terra e del Mare (DiSTeM), Università degli Studi di Palermo, Palermo, Italy
(4) Department of Biology, Ecology and Earth Sciences (DiBEST), Università della Calabria, Italy
(5) Institut de Physique du Globe de Paris (IPGP), Université de Paris, Paris, France
(6) Laboratoire Interuniversitaire des Systèmes Atmosphériques (LISA), Université Paris-Est-Créteil, Université de Paris, Institut Pierre Simon Laplace (IPSL), Créteil, France

HIGHLIGHTS

- Sulphate black crusts are mostly collected on carbonate building stones from different environments (coastal, rural, urban and volcanic environments).
- $\delta^{34}S$ and $\delta^{18}O$ indicate that black crust sulphur is mostly derived from anthropogenic sources.
- $\Delta^{33}S$ and $\Delta^{36}S$ of black crust sulphate are distinct from those of atmospheric sulphate aerosols.
- The largest $\Delta^{17}O$ anomalies are measured in black crust sampled in locations downwind of an active volcano (Mt Etna).

GRAPHICAL ABSTRACT

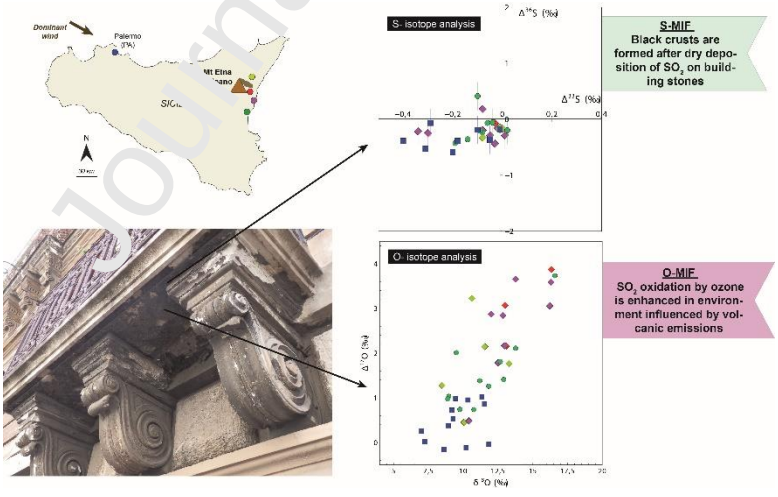

Abstract

The deterioration of monument or building stone materials is mostly due to the growth of black crusts that cause blackening and disaggregation of the exposed surface. This study reports on new oxygen ($\delta^{17}O$, $\delta^{18}O$ and $\Delta^{17}O$) and sulphur ($\delta^{33}S$, $\delta^{34}S$, $\delta^{36}S$, $\Delta^{33}S$ and $\Delta^{36}S$) isotopic analyses of black crust sulphates formed on building stones in Sicily (Southern Italy). The measurements are used to identify the possible influence of volcanic emissions on black crust formation. Black crusts were mostly sampled on carbonate stone substrate in different locations subject to various sulphur emission sources (marine, anthropogenic and volcanic). Unlike atmospheric sulphate aerosols that mostly exhibit $\Delta^{33}S > 0‰$, here most of the analysed black crust sulphates show negative $\Delta^{33}S$. This confirms that black crust sulphates do not result from deposition of sulphate aerosols or of rainwater but mostly from the oxidation of dry deposited SO_2 onto the stone substrate. The $\delta^{34}S$ and $\delta^{18}O$ values indicate that most of black crust sulphate originates from anthropogenic activities. $\Delta^{17}O$ values are found to be related to the sampling location. The largest ^{17}O anomalies (up to ~4‰) are measured in black crust from areas highly influenced by volcanic emissions, which demonstrates the strong involvement of ozone in the formation of black crusts in volcanically influenced environments.

Keywords: stone degradation, black crust, sulphur isotope, oxygen isotope, $\Delta^{17}O$ anomaly, volcanic emissions.

* corresponding author.
E-mail address: adeline.aroskay@sorbonne-universite.fr
4 Place Jussieu, 75005, Paris (France)

1. Introduction

"Black Crusts" are micrometric to centimetric thick black layers observed on the surface of buildings, monument walls or sculptures (Figure 1). They represent one of the main studied cause of carbonate stone deterioration and cultural heritage damage in urban environments (Winkler, 1966; Longinelli & Bartelloni, 1978; Del Monte et al., 1981; Camuffo et al., 1982; Camuffo et al., 1983; Huneef et al., 1992; Sabbioni, 1995; Torfs et al., 1997; Ausset et al., 1999; Massey, 1999; Ausset & Lefevre, 2000; Bugini et al., 2000; Cardell-Fernández et al., 2002; Charola & Ware, 2002; Vallet et al., 2006; Lefèvre et al., 2007; Montana et al., 2008; Fronteau et al., 2010; Török et al., 2010; Barca et al., 2011; Kloppmann et al., 2011; Kramar et al., 2011; Livingston, 2012; Montana et al., 2012; Ruffolo et al., 2015; Steiger, 2016; Bonazza & Sabbioni, 2016; Comite et al., 2017; Pozo-Antonio et al., 2017; Comite & Fermo, 2018; La Russa et al., 2018, 2017; Farkas et al., 2018; Genot et al., 2020). In present-day polluted urban areas, black crusts are mostly found on surfaces partly shielded from rainfall, but still humid (Camuffo et al., 1982; Camuffo et al., 1983, Massey, 1999). The crust structure is mainly composed of gypsum crystals ($CaSO_4 \cdot 2H_2O$) with entrapped atmospheric

particles such as fly-ash and soot which cause the blackening (Del Monte et al., 1981; Ausset et al., 1998; Fronteau et al., 2010).

Although a fraction of airborne gypsum can be incorporated in the deterioration layer (Davis, 1981; Camuffo et al., 1983), black crusts are the result of authigenic precipitation of gypsum on carbonate stone surfaces due to the chemical reaction between sulphate (SO_4^{2-}) and calcite ($CaCO_3$). This chemical reaction, called sulphatation (Camuffo et al., 1982) or sulphation (Ausset & Lefevre, 2000; Lefèvre et al., 2007) might also be catalysed by the carbonaceous particles formed during the incomplete burning of oil or coal (Novakov et al., 1974; Britton & Clarke, 1980; Cofer et al., 1980; Cofer et al., 1981; Ausset et al., 1999). Black crusts are considered to be good traps for atmospheric particles. As such, their study allows to better identify the particulate pollution emission sources in urban areas (Ausset et al., 1998; Del Monte et al, 2001; Lefèvre & Ausset, 2002). Some insights into sulphur emissions sources in polluted urban areas were also gained from their isotopic composition ($\delta^{34}S$ and very few $\delta^{18}O$) (Buzek & Šrámek, 1985; Nyo & Schiavon, 1989; Kramar et al., 2011; Montana et al., 2008, 2012). Following previous studies of natural sulphate-containing samples such as aerosols, rainwaters, ice cores or volcanic deposits (Bao et al., 2000; Lee et al., 2001a; Romero et al., 2003; Jenkins et al., 2006; Mather et al., 2006; Sofen et al., 2011; Alexander et al., 2012; Martin, 2018), Geniot et al. (2020) reported recently on the first oxygen and sulphur multi-isotopic composition measurements of sulphate from black crust ($\delta^{18}O$, $\delta^{34}S$, $\Delta^{17}O$, $\Delta^{33}S$ and $\Delta^{36}S$).

Atmospheric oxidants, such as O_3, H_2O_2, OH and O_2-TMI (O_2 catalysed by Transition Metal Ion) indeed carry specific oxygen mass-independent fractionation signatures (O-MIF; $\Delta^{17}O \neq 0‰$) that are inherited from the ozone molecule precursor. When a sulphur gas (e.g. SO_2) is oxidized, part or all of the oxidant-specific ^{17}O-anomaly is transferred to the sulphate product. Consequently, the $\Delta^{17}O$ measured in sulphate can be used as a tracer of sulphur oxidation pathways in the atmosphere (Savarino et al., 2000). In addition to O-MIF signatures, there have been attempts to use multi-sulphur isotope measurements ($\Delta^{33}S$ and $\Delta^{36}S$) as oxidation

pathway tracers (Harris et al., 2012a; Harris et al., 2012b; Harris et al., 2013a; Harris et al., 2013b; Au Yang et al., 2018), including atmospheric photochemical processes (Farquhar et al., 2000; Farquhar et al., 2001; Farquhar & Wing, 2003). However, interpretations of multi-sulphur isotopic data in atmospheric sulphate aerosols remain challenging (Guo et al., 2010; Au Yang et al., 2018; Au Yang et al., 2019).

The only investigation into the origin of sulphate in black crusts using a multi-isotopic oxygen and sulphur approach was conducted by Genot et al. (2020). Black crusts were sampled in the Parisian Basin (France) according to a NW-SE cross-section, covering from rather suburban to more polluted environments in the heart of the Paris megapolis. Unexpected MIF isotopic compositions ($\Delta^{17}O$ up to 2.56‰, -0.34‰ < $\Delta^{33}S$ < 0‰ and $\Delta^{36}S$ ~ -0.4‰) were measured. Based on O isotopes and $\delta^{34}S$, Genot et al. (2020) proposed that sulphate from Parisian black crusts mostly originate from the oxidation of anthropogenic sulphur gases by H_2O_2. Furthermore, they also suggested that a magnetic isotope effect during the formation of black crust sulphate might be responsible for the very unusual S-MIF signature. Since black crusts were only sampled in the Parisian Basin, it is not clear whether these singular isotopic compositions are common to all black crusts in the world or simply characteristic of the Paris megapolis.

The present work builds on the Genot et al. (2020) study using the same isotopic approach. It deals with the formation of black crust all over Sicily (Italy) instead of the Parisian Basin (France). Although most of the sulphur sources in Sicily are anthropogenic and marine, as in the Parisian Basin, the strengths and mix of emission sources in Sicily and in the Parisian Basin are very different, resulting in differences in atmospheric chemical reactivity and hence possibly sulphur oxidation. It is therefore essential to understand whether sulphur oxidation processes driving the black crust formation in Sicily are the same as in the Parisian area. More interestingly, some of the areas sampled in Sicily are downwind of the Mount Etna volcano and hence under the strong influence of volcanic emissions, giving the opportunity to extend the black crust isotopic characterisation to a new environment. Indeed, Mount Etna

presents a quasi-permanent activity with an almost continuous passive degassing punctuated with regular eruptive phases (average volcanic SO_2 emissions ~ 5500 $Mg.day^{-1}$) (Aiuppa et al., 2001, 2005; Scollo et al., 2009; Calabrese et al., 2011). This offers the opportunity of exploring the potential effect of volcanic emissions on the formation of black crusts, notably the relative importance of different sulphur oxidation processes.

2. Material and Methods

2.1. Sampling strategy

Black crusts were sampled in Sicily, overwhelmingly on building stones made of highly porous carbonate rocks (calcarenite, Fig.1). Few black crust samples were also collected on lime-based mortar or plaster, and basalt stone substrates. As discussed below, their isotopic composition is consistent with the rest of all the samples, therefore they are not discussed separately in the paper. In the city of Palermo, 13 samples were collected, while 20 samples were collected in the city of Catania and 23 others in the eastern region of the Mount Etna Volcano, in or very close to the towns of Acireale, Linguaglossa, and Zafferana Etnea. Most of the monuments on which black crusts were sampled were built during the pre-industrial period, but information about the construction year of private buildings remain scarce. Overall, collected black crusts were formed between the pre-industrial period and the present day. Most of the black crusts sampled are sub-millimetric to millimetric thick. Detailed locations and substrates on which black crusts were sampled are summarised in table 1. Each area represents an environment influenced by a specific mix of emissions. Due to its proximity with the Mediterranean Sea and its urbanisation, Palermo city is mainly under the influence of marine and anthropogenic emissions (Comite et al., 2017; Varrica et al., 2019). Catania, Acireale, Linguaglossa and Zafferana Etnea are subject not only to marine and anthropogenic emissions, but also to volcanic emissions (Barca et al., 2011; Lanzafame et al., 2014; Andronico & Del Carlo, 2016) depending on the prevailing wind direction and their proximity to the Etna volcano. Since the main wind direction is NW-SE, the Acireale and Zafferana Etnea areas are likely more influenced by volcanic emissions than Catania and

Linguaglossa. On the contrary, Palermo should be not influenced by volcanic emissions at all (Fig.1). All the samples were collected on walls at height higher than 1.5m to prevent capillary rising from the ground and only the black part of the crust was collected trying to prevent significant substratum contamination.

2.2. Anionic content and sulphate purification

The anionic content was measured at the ISTeP geochemical laboratory (Paris, France) using an anion chromatography (Dionex ISC 110, Thermo Scientific) calibrated for SO_4^{2-}, NO_3^- and Cl^- ions. This chemical analysis was conducted after crushing, leaching in deionized water and filtering down to 0.45µm between 30 and 100mg of black crust. The replication of the measurements gives a reproducibility of 0.3 ppm, 0.4 ppm and 0.1 ppm for sulphate, nitrate and chlorine ion concentrations, respectively. The sulphate is then extracted from the black crust leachate, concentrated, and purified according to the anion-exchange resin method developed and described by Le Gendre et al. (2016). At least 10 mg of barium sulphate (barite) is finally precipitated in order to comfortably proceed to O- and S-multi-isotopic analyses.

2.3. O- and S-multi-isotopes analyses

Oxygen and sulphur multi-isotopic analyses on sulphate were performed at the IPGP Stable Isotope Laboratory (Paris, France).

O-multi-isotopic analyses were performed using the laser fluorination method (Bao & Thiemens, 2000) on 2-4mg of barite ($BaSO_4$). After fluorination of the sample under 40 Torr of BrF_5, extracted O_2 is purified through a series of liquid nitrogen and slush traps and collected on a molecular sieve. The purified O_2 is then injected into a Delta-V Isotope Ratio Mass Spectrometer (Thermo Fischer Scientific, Bremen, Germany) and run in dual inlet to monitor the m/z: 32, 33 and 34 which are then used to determine the $\delta^{17}O$ and $\delta^{18}O$. The $\Delta^{17}O$ is calculated according to the following expression (Bao et al., 2016) :

$$\Delta^{17}O = \delta^{17}O - [(\delta^{18}O + 1)^{0.5305} - 1]$$

Since O_2 extraction from barite via the fluorination process is not complete (yield of ~40% on the samples from this study), mass-dependent isotopic fractionation occurs, which means that measured $\delta^{18}O$ and $\delta^{17}O$ are different from $\delta^{18}O$ and $\delta^{17}O$ in barite, whereas the $\Delta^{17}O$ is not affected by these fractionation processes. The measured $\delta^{18}O$ values thus require correction using the NBS 127 international standard as a reference. Measured $\delta^{18}O$ and $\Delta^{17}O$ values for NBS 127 are 0.4 ± 0.2‰ and 0.04 ± 0.01‰ (confidence interval (CI) in 2σ, n=42), respectively. Assuming a standard certified $\delta^{18}O$ value of 8.6‰ for the NBS 127, the samples $\delta^{18}O$ were systematically corrected according to the NBS127 standards from the same analytical session. Based on sample replicates from this study, the global reproducibility for $\delta^{18}O$ and $\Delta^{17}O$ (integrating the uncertainties derived from the sulphate extraction method, the fluorination line and the mass spectrometer) is usually lower than 1.0‰ and 0.1‰ (1 standard deviation; 1σ) respectively.

For S-isotope analyses, barite samples ($BaSO_4$) were reduced into H_2S and precipitated in Ag_2S following the protocol described in Thode et al. (1961). Silver sulphide was then rinsed three times with Millipore water and dried at 70°C overnight before being placed into Ni-reaction bombs for fluorination to produce SF_6 according to Farquhar et al. (2007); Labidi et al. (2012). The purified SF_6 was analysed using an isotope ratio mass spectrometer (ThermoFinnigan MAT-253) running in dual inlet mode, to monitor m/z: 127, 128, 129 and 131 used to determine $\delta^{33}S$, $\delta^{34}S$, and $\delta^{36}S$. The $\Delta^{33}S$ and $\Delta^{36}S$ are calculated according to the following expressions (Farquhar & Wing, 2003) :

$$\Delta^{33}S = \delta^{33}S - [(\delta^{34}S + 1)^{0.515} - 1]$$

$$\Delta^{36}S = \delta^{36}S - [(\delta^{34}S + 1)^{1.89} - 1]$$

$\delta^{34}S$-values are measured against the in-house SF_6 tank that has been calibrated with respect to the IAEA-S1 international standard ($\delta^{34}S_{(IAEA\text{-}S1)}$ = -0.3‰ vs CDT). Following Defouilloy et al. (2016), all our $\Delta^{33}S$ and $\Delta^{36}S$ values are also given with respect to CDT by correcting the initial $\Delta^{33}S$ and $\Delta^{36}S$ values, initially expressed with respect to the in-house SF_6 tank, with a factor of +0.029 and +0.129‰ respectively.

Repeated analyses of the IAEA-S1 internal standard give values of -0.29 ± 0.03; 0.084± 0.004 and -0.881 ± 0.097 (Confidence Interval (CI) in 2σ, n=14) for $\delta^{34}S$, $\Delta^{33}S$ and $\Delta^{36}S$ respectively.

Based on in-house standard replicates, the reproducibility that integrates the uncertainties derived from the barite reduction step, the purification line and the mass spectrometer is 0.5, 0.009 and 0.06 (CI in 2σ, n=9) for $\delta^{34}S$, $\Delta^{33}S$ and $\Delta^{36}S$ respectively. Finally, based on 4 duplicates from this study, the global reproducibility for $\delta^{34}S$, $\Delta^{33}S$ and $\Delta^{36}S$ (integrating the uncertainties derived from the sulphate extraction method, the barite reduction step, purification line and the mass spectrometer) is estimated to be 0.8‰, 0.01‰ and 0.20 (1σ) respectively.

2.4. SEM-EDS analysis

Scanning Electron Microscopy (SEM) coupled with Energy Dispersive X-ray Spectroscopy (EDS) were used to produce high resolution images in order to acquire details about the microstructure of the black crusts with the image analysis giving some crude estimations about their elemental composition. SEM-EDS analyses were conducted at the ISTeP Laboratory with a ZEISS Supra 55 VP – microscope (Sorbonne Université, Paris) and at the ATeN Center Laboratory with a Thermo Fischer Scientific PHENOM PROX desktop SEM (University of Palermo).

3. Results

3.1. Anionic content of black crusts

Chromatography analyses confirm that in most black crust samples, sulphates represent the major anionic species, they also reveal the presence of significant amounts of nitrate and chlorine (see Table 4 in supplementary material IV). Concentration measurements are reported as mass mixing ratios, i.e. ratios of the mass of a specific anion to the mass of black crust leached in the sample analysed. The values range between 33563 and 278831 ppm for sulphate, 0 and 91904 ppm for nitrate, and 207 and 5032 ppm for chlorine. No correlation is

observed between the concentrations of the different anions (see Fig.9 in supplementary material III). Nevertheless, differences between anionic concentration at different sampling locations can be seen. The chlorine concentrations are the highest for black crusts from the most coastal cities with mean concentrations of 3118 ppm for Palermo, 2524 ppm for Acireale and 1815 ppm for Catania. The nitrate concentrations are the highest for black crusts from the largest cities with mean concentrations of 3271 ppm for Catania (note that the outlier of 91904 ppm was removed to calculate the average concentration), 3221 ppm for Palermo, and 2139 ppm for Acireale. Despite the care taken to collect only the black part of the crust, especially at the substratum/crust interface, the possibility of having collected a non-negligible fraction of substratum in some samples cannot be excluded. As much larger amounts of sulphate, nitrate and chlorine are expected in black crust than in the substratum, measured concentrations in black crust samples reported here necessarily correspond to the lowest limits for anionic concentrations. Since the measured concentrations in other studies (Montana et al., 2008, 2012; Török et al., 2010; Comite et al., 2017; Comite & Fermo, 2018; La Russa et al., 2017, 2018) are not always compared to the mass of black crust, the direct comparison of absolute concentrations from the literature is not possible. Therefore, in the rest of the paper, only ratios of anion concentrations will be discussed.

3.2. Scanning Electron Microscopy (SEM) analyses

The micromorphology and composition of black crusts were studied by means of SEM observations and Energy Dispersive X-ray Spectrometry (EDS). Figure 2 shows examples of SEM images obtained for black crusts from various sampling sites, especially samples from Palermo (PA-10 and PA-6), from Catania (CT-5) and from Zafferana Etnea (ZAF-4). Gypsum crystals of various sizes and morphologies are found in all the samples (red arrows on Fig. 2). More widespread are chaotic aggregates formed by microcrystals (1-5µm) with mainly irregular morphology (Fig. 2a and 2c). In the samples examined, gypsum is also common in the form of rose-like aggregates of tabular-lenticular crystals (20-70 µm) (Fig. 2b and 2e). Parallel aggregates of regular prismatic crystals (10-20 µm) are detected more sporadically.

The samples from all the sites also contain halite crystals and some NaCl precipitation. These halite crystals occur in the form of euhedral (cubic) crystals, often deliquescent, that are, as cryptocrystalline and very compact masses, dispersed within the gypsum anhedral microcrystals. Both salt precipitation and halite crystals are more frequent in Palermo samples (Fig. 2b, 2c and 2d) which indicates a stronger influence of marine emissions, consistent with the current prevailing wind direction (from North-West to South-East) blowing from the sea. Metallic particles and iron oxide particles generated during fuel combustion are also observed in all the samples (Fig. 2a and 2b), confirming the importance of anthropogenic emissions at all the sites. Black crusts sampled at Catania, Acireale, Linguaglossa and Zafferana Etnea appear to contain many silicate particles, such as olivine, plagioclase, pyroxenes and titano-magnetite crystals and also mostly volcanic glass shards that are more or less altered (Fig. 2e, 2f, 2g and 2h). Volcanic glass shards appear to be relatively less frequent in Catania and Linguaglossa samples, while they are totally absent in Palermo samples. These results are fully consistent with the expected influence of volcanic emissions on the different areas, with Zafferana Etnea and Acireale being close and often downwind from the Etna volcano, in agreement with the direction of the prevailing winds (high volcanic influence), Catania and Linguaglossa being close and sporadically downwind from the Etna (lower volcanic influence), and Palermo being far from and upwind of the Mount Etna (no volcanic influence). Overall, the black crust samples from Sicily contain gypsum, calcite, and halite crystals as well as particles inherited from fuel combustion processes. Only the black crusts sampled downwind from the Etna volcano differ from the other samples with the abundant presence of volcanic particles. These observations are consistent with other reported SEM analyses for Sicilian and European black crusts (Bugini et al., 2000; Barca et al., 2011; Farkas et al., 2018; Montana et al., 2008, 2012).

3.3. Sulphur and oxygen isotopic analyses

The $\delta^{18}O$ values measured in black crust samples vary from 7.2‰ up to 16.6‰ while $\Delta^{17}O$ ranges from -0.17‰ to 3.82‰ (Table 2). Overall, our $\Delta^{17}O$ values are positively correlated to

the $\delta^{18}O$ values (R^2=0.62) (Fig.3); with different data groups corresponding to different sampling areas being distinguishable. The first group (group 1; Fig.3) consists of samples from Palermo and is characterised by the lowest values. $\Delta^{17}O$ ranges from -0.17‰ to 1.00‰ with a mean of 0.44‰ ± 0.26 and $\delta^{18}O$ ranges from 7.2‰ to 11.8‰ with a mean of 9.6‰ ± 0.9 (CI in 2σ; n=12 for both). The second group (group 2; Fig.3), which has intermediate values, appears to correspond mostly to samples from Catania and Linguaglossa. $\Delta^{17}O$ values from Catania range from 0.72‰ to 3.68‰ with a mean value of 1.54‰ ± 0.50 and $\delta^{18}O$ values range from 8.9‰ to 16.6‰ with a mean value of 11.5‰ ± 1.4 (CI in 2σ; n=12). Note that only one sample shows rather high $\Delta^{17}O$ and $\delta^{18}O$ values of 3.68‰ and 16.6‰ respectively, with the second highest $\Delta^{17}O$ and $\delta^{18}O$ values being 2.08‰ and 13.8‰ respectively. $\Delta^{17}O$ values from Linguaglossa range from 0.44‰ to 3.20‰ with a mean value of 1.75‰ ± 0.9 and $\delta^{18}O$ values range from 10.1‰ to 13.3‰ with a mean value of 10.8‰ ± 1.6 (CI in 2σ; n=5). The third group (group 3; Fig.3), which shows the highest values, consists of samples from Zafferana and Acireale. $\Delta^{17}O$ values from Zafferana range from 2.13‰ to 3.82‰ with a mean value of 3.00‰ ± 0.96 and $\delta^{18}O$ values range from 13‰ to 16.3‰ with a mean value of 14.1‰ ± 2.1 (CI in 2σ; n=3). $\Delta^{17}O$ values from Acireale range from 0.47‰ to 3.62‰ with a mean value of 2.52‰ ±0,72 and $\delta^{18}O$ values range from 10.4‰ to 16.3‰ with a mean value of 13.4‰ ± 1.4 (CI in 2σ; n=8). These three groups correspond to geographical areas influenced by different contributions from emission sources. If all areas are subject to anthropogenic and marine emissions, the influence of volcanic emissions increases gradually from group 1 to 3. Indeed, the mean wind direction indicates that volcanic emissions do not affect the Palermo area (group 1), while the Acireale and Zafferana areas (group 3) are often downwind of the Mount Etna volcano, right in the prevailing wind direction (Fig. 1). The Catania and Linguaglossa areas (group 2) are more sporadically affected by volcanic emissions.

Measured $\delta^{34}S$ values range from -2.68‰ to 15.04‰ (Table2; Fig.4). Samples from Palermo show $\delta^{34}S$ values ranging from -2.68‰ to 5.10‰ with a mean value of 0.9‰ ± 1.6 (CI in 2σ;

n=9). Samples from Catania show $\delta^{34}S$ values ranging from -1.64‰ to 9.13‰ with an average value of 4.0‰ ± 2.2 (CI in 2σ; n=8). Black crust from Linguaglossa show $\delta^{34}S$ values ranging from -0.74‰ to 15.04‰ with an average value of 6.4‰ ± 5.7 (CI in 2σ; n=5) and samples from Acireale show $\delta^{34}S$ values ranging from -1.74‰ to 5.56‰ with an average value of 1.8‰ ± 2.1 (CI in 2σ; n=8).

$\Delta^{36}S$ values for all the samples range from -0.59‰ to 0.41 ‰ with a mean value of -0.23 ‰ ± 0.2 (1σ; ±0.04 for the CI in 2σ), whereas $\Delta^{33}S$ values range from -0.4‰ to 0.02‰ with a mean value of -0.11 ‰ ± 0.11 (1σ; ±0.07 for the CI in 2σ; Table 2; Fig.5). Note that the global reproducibility based on 4 sample duplicates on $\Delta^{36}S$ measurements is ±0.20‰ (1σ), which suggests that variability in $\Delta^{36}S$ observed in our dataset is rather insignificant. Consequently, in the following discussion, the $\Delta^{36}S$ is considered as relatively constant. In contrast, the global reproducibility based on 4 sample duplicates from this study on the $\Delta^{33}S$ is ±0.01‰ (1σ), which is one order of magnitude lower than the variability observed in our dataset. Therefore, the variability observed in the $\Delta^{33}S$ is clearly significant. Finally, no correlation is found between the sulphur isotopic composition and the sampling areas (Fig.4 and 5), which is drastically different from the results obtained for the oxygen isotopes (Fig. 3).

4. Discussion

4.1. The origin of sulphur from black crusts

4.1.1. Anthropogenic emissions as the main contributor of sulphur to black crusts

The $\delta^{34}S$ and $\delta^{18}O$ signatures measured in black crusts from Sicily range from -2.68‰ to 15.04‰ (mean value: 2.8‰ ±1.4; CI in 2σ; n=31) and from 7.2‰ to 16.6‰ (mean value: 11.4 ± 0.8‰; CI in 2σ; n=40), respectively (Table 2, Fig.4). In Sicily, the main S-sources are anthropogenic from fuel combustion and marine emissions, as well as volcanic emissions in the eastern part of Sicily (Fig. 1). The contribution of endogenous sulphates from the stone wall is an additional potential source. SEM analyses (Fig.2) also indicate that different sources contribute to the formation of black crusts according to their geographical positions

with respect to the Etna volcano. Halite crystals (Fig.2b, 2c and 2d) from marine emissions and metallic particles (Fig. 2a and 2b) from fuel combustion are observed entrapped in the gypsum crust in all the samples whereas volcanic particles (Fig. 2e, 2f, 2g and 2h) are also present in samples from the eastern part of Sicily. The confrontation of the isotopic values from Sicilian black crusts with the $\delta^{34}S$ and $\delta^{18}O$ signatures of various sulphur emission sources, further supports the influences of the aforementioned sulphur sources. Anthropogenic sulphur emissions show the largest range of isotopic values with $\delta^{34}S$ values spanning from -30‰ for sulphur from coal combustion (Rees, 1970) to 32‰ for sulphur from coal and petroleum combustion (Smith & Batts, 1974), and a narrower range of $\delta^{18}O$ values from ~5‰ to ~11‰ (Lee et al., 2002). Magmatic sulphur species show $\delta^{34}S$ and $\delta^{18}O$ values ranging from -1‰ to 6‰ and from ~5‰ to 7‰ respectively (De Hoog et al.,2001; Eiler, 2001; Labidi et al., 2012). Endogenous (intrinsic) sulphates that come from carbonate associated sulphate (CAS, in the carbonate stone) and from the wall plaster have specific isotopic signatures. CAS $\delta^{34}S$ and $\delta^{18}O$ range from ~ 12‰ to ~21‰ and from 5‰ to ~20‰ respectively (Turchyn et al., 2009; Pennie & Turchyn, 2014). In Europe, $\delta^{34}S$ values in sulphate from wall plaster range from ~ 12‰ to ~18‰ and $\delta^{18}O$ values range from ~ 14‰ to 20‰ (Kloppmann et al., 2011; Fig 4). $\Delta^{17}O$ values of endogenous sulphates are close to 0‰ or even slightly negative (Bao et al.,2008). In contrast, $\Delta^{17}O$ values of most of our Sicilian black crusts are > 0‰ (Table 2; Fig.3). Therefore, even if black crust $\delta^{34}S$ and $\delta^{18}O$ compositions could reflect the contribution of endogenous sulphates, our $\Delta^{17}O$ signatures are not consistent with an important intrinsic origin. For this reason, endogenous sulphate should represent a minor source of sulphur and will be neglected thereafter. From their geographical locations, each sampling area is subject to diverse sulphur emission sources whose relative contributions can be estimated from their average $\delta^{34}S$ value. From its location and urbanization, Palermo represents the sampling site the most influenced by anthropogenic and marine emissions. The mean $\delta^{34}S$ value of 0.9‰ measured in black crusts from this coastal urban area is most likely the result of a mixing between anthropogenic sulphur and marine sulphur, with the high $\delta^{34}S$ signature of marine sulphur (~ 21‰) being diluted by the

low $\delta^{34}S$ anthropogenic sulphur. Indeed, if a mean value of 0‰ for the $\delta^{34}S$ of anthropogenic sulphur is considered, the mean anthropogenic contribution can be estimated to be ~95% and a marine contribution of ~5% (see supplementary material I for calculation details). The larger input of anthropogenic sulphur is fully consistent with the mean $\delta^{34}S$ signature of 2.1‰ measured by Montana et al. (2008 in black crusts from Palermo which is explained by an anthropogenic contribution of ~90%. In an area, where anthropogenic, marine but also volcanic influences are significant, such as Acireale (Fig. 1), the black crusts have a mean $\delta^{34}S$ value of 1.8‰. Overall, the marine contribution seems to be rather marginal in all the black crust samples, even in coastal locations. Assuming that it is of the order of about 5%, the mean $\delta^{34}S$ value of 1.8‰ measured in black crusts from Acireale can be explained by ~76% of anthropogenic sulphur ($\delta^{34}S$ = 0‰), ~19% of volcanic sulphur ($\delta^{34}S$ = 4‰) and ~5% of marine sulphur ($\delta^{34}S$ = 21‰; see supplementary material I for calculation details). It is worth noting that even if the volcanic sulphur contributes significantly to the black crust $\delta^{34}S$ signature, the anthropogenic emissions remain easily the dominant source of sulphur for the black crust.

The similarity between the isotopic values (especially the $\delta^{34}S$) from Sicilian black crusts (this study) and those from other cities in Europe (Longinelli & Bartelloni, 1978; Buzek & Šrámek, 1985; Pye & Schiavon, 1982; Torfs et al., 1997; Siedel, 2000; Klemm & Siedel, 2002; Přikryl et al., 2004; Vallet et al., 2006; Kloppmann et al., 2011; Genot et al., 2020) suggests that similar sulphur sources contribute to the formation of their black crusts. This study thus confirms that in large urban areas, the black crust formation mostly results from anthropogenic sulphur emissions (Winkler, 1966; Massey, 1999; Bugini et al., 2000; Cardell-Fernández et al., 2002; Charola & Ware, 2002; Lefèvre & Ausset, 2002; Holynska et al., 2004; Přikryl et al., 2004; Barca et al., 2011; Kramar et al., 2011; Comite & Fermo, 2018; Farkas et al., 2018; La Russa et al., 2018; Genot et al., 2020). More interestingly, the present work broadens the study of black crusts to different and various atmospheric environments (urban, coastal, rural and volcanic areas), and show that anthropogenic emissions still

remain the main source of black crust sulphur. Now it is important to explore whether this anthropogenic sulphur contribution originates from sulphur gas (SO_2) or sulphate aerosols (H_2SO_4).

4.1.2. Black crusts mostly originate from dry deposition of SO_2 and not atmospheric sulphate aerosols

The multi-sulphur isotopic analyses performed on black crusts from different atmospheric environments (urban, rural, coastal and volcanic areas) in Sicily show very singular $\Delta^{33}S$ and $\Delta^{36}S$ signatures (Table 2, Fig. 5), characterized by a significant $\Delta^{33}S$ variability, from -0.4‰ to 0.02‰, and a relatively constant $\Delta^{36}S$ (see section 3.3). Such negative $\Delta^{33}S$ signatures associated with relatively constant $\Delta^{36}S$ values are also observed in black crusts from the Parisian Basin by Genot et al. (2020). Recent studies on sulphate aerosols also reported unexpected negative $\Delta^{33}S$ in other natural sulphur compounds (Lee et al., 2002; Shaheen et al., 2014; Han et al., 2017; Lin et al., 2018). This was tentatively attributed to an additional MIF process occurring during fossil fuel combustion and associated primary sulphate formation. To our best knowledge, black crusts remain the only natural sulphur compounds showing systematic negative $\Delta^{33}S$ (associated to a constant $\Delta^{36}S$), which makes them unique in that respect. Hence, sulphate from black crust certainly has a different origin from the atmospheric sulphate aerosols that are overwhelmingly characterized by positive $\Delta^{33}S$ (Fig.5). Two implications result from this observation. First, black crust sulphates cannot originate from the dry or wet deposition of atmospheric sulphate on the wall. Instead they mostly result from the dry deposition of atmospheric SO_2 and its subsequent oxidation into sulphate on the stone wall. Secondly, a mass-independent process must occur during oxidation to create ^{33}S depletion measured in black crust sulphates. Genot et al. (2020) propose the existence of a Magnetic Isotope Effect (MIE; Buchachenko, 2001) that affects only odd isotopes between the SO_2 deposition on the wall surface and its oxidation into sulphate. Although this isotopic effect is still rather speculative and requires laboratory

experiments to characterise the exact mechanism, it provides a way to comply with two important conditions in order to explain our isotopic data: the generation of a positive $\Delta^{33}S$ and a negative $\Delta^{33}S$ sulphur pools and their physical separation. Therefore, the oxidation of SO_2 in interaction with the wall under the MIE has to be accompanied by a reaction leading to the formation of gypsum, physically separating the residual SO_2 (positive $\Delta^{33}S$) and black crust sulphate (negative $\Delta^{33}S$). Furthermore, since the wall surface is a humid environment, it is very likely that the oxidation of SO_2 takes place in an aqueous-like environment such as a thin liquid water film on the mineral surfaces (Massey, 1999; Klemm & Siedel, 2002; Behlen et al., 2008; Corvo et al., 2010; Wiese et al., 2013). This aqueous oxidation is highly unlikely to be identical to that occurring in the atmosphere, where no MIE is expected. Nonetheless, the black crust O-MIF signature is still expected to be mostly determined by the isotopic signatures of the different oxidants involved in black crust sulphate formation rather than by the MIE (Genot et al., 2020).

Finally, our results confirm the singular multi S-isotope composition of black crusts measured in large urban areas, but they also indicate that this isotopic feature is rather an intrinsic characteristic to black crust formation, whatever its atmospheric environment during its formation (urban, rural, coastal or volcanic areas).

The $[SO_4^{2-}]/[Cl^-]$ ratios for black crusts from the different Sicilian and other European sampling sites range from a few tens (~40) to hundreds (~200), values which are at least two orders of magnitude higher than the Palermo rainwater $[SO_4^{2-}]/[Cl^-]$ of 0.24 on average and the Etnean area rainwater average $[SO_4^{2-}]/[Cl^-]$ of 0.99 (Fig.6). Although this difference between black crusts and the local rainwaters can result from a preferential incorporation of sulphates over chlorine into the crust, leading to higher $[SO_4^{2-}]/[Cl^-]$ ratios, it can also be interpreted as the rainwater sulphate being a very marginal source of sulphate in black crust. Moreover, if aerosol deposition was the dominant process in the formation of black crust, some correlation between sulphate and nitrate in black crust could be expected from sulphate and nitrate ratios in aerosols. The actual absence of correlation is an additional

indication that black crusts do not derive from aerosol deposition. This is consistent with the dry deposition of SO_2 followed by its oxidation on the stone wall being the dominant source of black crust sulphate, as attested by the $\Delta^{33}S$ and $\Delta^{36}S$ signatures discussed above. Furthermore, this mechanism is confirmed by the abundant literature on building stone deterioration which considers the dry deposition of air pollutants such as SO_2 to be the dominant mechanism in stone decay (Roekens & van Grieken, 1989; Girardet & Furlan, 1989; Ausset et al., 1999; Massey, 1999; Cardell-Fernández et al., 2002; Charola & Ware, 2002; Holynska et al., 2004; Livingston, 2012; Steiger, 2016; Bonazza & Sabbioni, 2016).

The $\delta^{34}S$ and $\delta^{18}O$ measured in black crusts from Sicily confirm that anthropogenic emissions remain the dominant contributor to sulphur in black crust, even in areas subject to other emission sources (see previous subsection 4.1.1). The $\Delta^{33}S$ and $\Delta^{36}S$ signatures and the $[SO_4^{2-}]/[Cl^-]$ ratios attest that anthropogenic sulphur that contributes to the formation of black crusts is very likely to originate, not in the deposition and accumulation of atmospheric sulphate aerosols, but mostly in the dry deposition of gaseous SO_2 from anthropogenic emissions, which is in agreement with previous studies (Massey, 1999; Behlen et al., 2008; Wiese et al., 2013).

4.2. Volcanic emissions influence the formation of black crusts in urban areas

4.2.1. High $\Delta^{17}O$ signatures in black crusts under volcanic emission influence

As shown in the previous section, our S-isotopic data confirms that black crust is formed predominantly from the deposition of gaseous SO_2 on the walls (see section 4.1). Our O-isotopic data provides some indications about the possible oxidants of deposited SO_2. One of the most interesting results of this study is that samples from the same area display similar O-isotope compositions and that these isotopic compositions are significantly distinct from one area to another (Fig. 3). Indeed, based on $\Delta^{17}O$ and $\delta^{18}O$, three groups corresponding to the main sampling areas can be identified (Fig. 3). Black crusts from Palermo, referred to as Group 1, show an average $\Delta^{17}O$ value of 0.44‰ ± 0.26 and a mean $\delta^{18}O$ value of 9.6 ± 0.9 (CI in 2σ; n=12). The second group is composed of black crusts from Catania and

Linguaglossa showing average $\Delta^{17}O$ values of 1.54‰ ± 0.50 (CI in 2σ; n=11) and 1.75‰ ± 0.9 (CI in 2σ; n=5) respectively and a mean $\delta^{18}O$ value of 11.5‰ ± 1.4 (CI in 2σ; n=11) and 10.8‰ ± 1.6 (CI in 2σ; n=5) respectively. Black crusts from Acireale and Zafferana compose the third group, showing average $\Delta^{17}O$ values of 2.52‰ ± 0.72 (CI in 2σ; n=8) and 3.00‰ ± 0.96 (CI in 2σ; n=3) respectively and a mean $\delta^{18}O$ value of 13.4‰ ± 1.4 (CI in 2σ; n=8) and 14.1‰ ± 2.1 (CI in 2σ; n=3) respectively. Such high $\Delta^{17}O$ values (up to 4‰; Table 2) have been reported in the literature, mostly for secondary volcanic sulphates related to Plinian and super-eruption events (Bao et al., 2000, 2001, 2003; Bao, 2005; Bindeman et al., 2007; Martin & Bindeman, 2009; Shaheen et al., 2013; Gautier et al., 2019) and in sea salt sulphates from the marine boundary layer (Alexander et al., 2005). Yet it is the first time that numerous $\Delta^{17}O$ values higher than 2.5‰ have been measured in black crusts.

$\Delta^{17}O$ measured in sulphates is expected to reflect the combined isotopic signatures of the dominant oxidation pathways involved in their formation. Indeed, each oxidant bears a specific ^{17}O anomaly that is partly transferred to the resulting sulphate. The expected O-isotope compositions for sulphates generated by each of the common atmospheric oxidation pathways have been experimentally determined by Savarino et al., (2000). In the gas-phase, the oxidation of SO_2 by OH-radicals leads to sulphates with a $\Delta^{17}O$ value of 0‰ in the troposphere because OH radicals are subject to a very rapid isotopic exchange with the abundant H_2O in the humid troposphere. In the aqueous phase, the oxidation by O_2-TMI ($\Delta^{17}O_{O2}$ ~ - 0.34‰) leads to sulphates with a $\Delta^{17}O$ value of -0.09‰. The oxidation by H_2O_2 ($\Delta^{17}O_{H2O2}$ ~ 1.70‰) leads to sulphates with a $\Delta^{17}O$ value of 0.87‰ and the isotopic anomaly in sulphates produced through the oxidation by O_3 is $\Delta^{17}O$ = 8.8‰ ($\Delta^{17}O_{O3}$ ~ 36‰; Galeazzo et al., 2018). It is noteworthy that, even if not well determined yet, the SO_2 oxidation by halogen compounds (HOX species such as HOBr and HOCl) could play a role in coastal environments (Monks et al., 2015; Chen et al., 2016). However, the produced sulphate is not expected to carry any MIF signatures (Chen et al., 2016), which makes these oxidation pathways indistinguishable from the O_2-TMI pathway. Therefore, in the estimated fraction of

SO_2 oxidized by O_2-TMI, it cannot be ruled out that some of the SO_2 was also oxidized by halogen species. In the following discussion, the O_2-TMI pathway essentially represents all the pathways that do not fractionate in a mass-independent way. Moreover, in polluted environments with high NOx levels, it has further been suggested that the oxidation of SO_2 by NO_2 may also represent a significant pathway (Steiger, 2016; Cheng et al., 2016; Au Yang et al., 2018). High $\Delta^{17}O$ values (between ~20‰ and ~40‰) can be generated in NOx (NO + NO_2) when ozone is involved in the NOx cycle (Morin et al., 2011; Michalski et al., 2013;). This ^{17}O anomaly may be transferred to the resulting sulphate during the oxidation of SO_2 by NO_2. However, this pathway remains very uncommon and the constraints on the oxygen isotopic transfer are limited. Therefore, this potential oxidation pathway is not considered here.

Since many $\Delta^{17}O$ values exceed 1‰ in our samples, O_3 must be strongly involved in the oxidation because, among the common SO_2 oxidants, it is the only one able to produce sulphate with $\Delta^{17}O>1‰$. Therefore, the SO_2 oxidation on the wall surface must take place in aqueous conditions, which rules out significant contribution of the gas-phase oxidation by OH-radicals. The homogeneity among the $\Delta^{17}O$ values of black crusts from the same sampling area indicates that different oxidation pathways are involved in black crust formation and contribute in similar proportions in each sampling area. Moreover, the positive correlation (R^2 = 0.62) between $\Delta^{17}O$ and $\delta^{18}O$ values (Fig.3) indicates that there is a transition in the SO_2 oxidation pathways budget from one extreme with both high $\Delta^{17}O$ and $\delta^{18}O$ values (>4‰ and >17‰ respectively) to another extreme with low $\Delta^{17}O$ and $\delta^{18}O$ values (<0‰ and <10‰ respectively). These two end-members represent the composition of sulphate produced through the aqueous oxidation of sulphur gases by the three prevalent pathways previously mentioned but in different proportions. Therefore, from the $\Delta^{17}O$ measured in black crusts from each group, the relative contributions of the 3 main oxidation pathways can be quantified as follows:

$$\Delta^{17}O(SO_4^{2-})_{measured} = f_{O2\text{-}TMI} \times \Delta^{17}O(SO_4^{2-})_{O2\text{-}TMI} + f_{H2O2} \times \Delta^{17}O(SO_4^{2-})_{H2O2} + f_{O3} \times \Delta^{17}O(SO_4^{2-})_{O3} \quad (R1)$$

with "*f*" representing the fluxes (relative contributions) of the different oxidation pathways. We assume that the sulphate produced by the oxidation of SO_2 by O_2-TMI, H_2O_2, and by O_3 generates a $\Delta^{17}O$ in sulphate of -0.09‰, 0.87‰ and 8.8‰ respectively (Galeazzo et al., 2018).

Table 3 shows for each group of black crusts the relative contributions of the different oxidation pathways. The most striking feature is that the ozone contribution increases from group 1 to group 3 with $f_{O3\text{-}group1}$ below 6% for group 1, $f_{O3\text{-}group2}$ ranging from 9% to 19% for group 2, and $f_{O3\text{-}group3}$ ranging from 22% and 31% for group 3 (Table 3), with f_{O3} value up to 44% for samples having the highest $\Delta^{17}O$ anomaly (~1 ‰).

The main difference between the atmospheric environments of the three black crusts groups is their respective degree of exposition to the Mt Etna volcanic emissions (Carn, 2005; Andronico et al., 2009; Scollo et al., 2009; Barca et al., 2011; Guerrieri et al., 2015; Andronico & Del Carlo, 2016). The 2 sites of group 3 are right in the path of the dominant winds (Fig.7, dark areas). The 2 sites of group 2 are rather on the edge of this dark area indicating that they are less exposed to winds blowing from Mt Etna. The site of group 1 (Palermo) is not exposed to winds blowing from Mt Etna. These observations are fully consistent with the findings of the SEM analyses, as indicated by the abundance of volcanic particles in black crusts from group 2 and 3 and their absence in group 1 (Fig. 2e, 2f, 2g and 2h).

Figure 7 clearly shows that the increase in black crust $\Delta^{17}O$ from groups 1 to 3, which is linked to an increase in the SO_2 oxidation by O_3, is positively correlated to relative contribution of volcanic emissions in the atmospheric environments. In standard urban areas such as Palermo and Paris areas, the average $\Delta^{17}O$ value measured in black crusts is 0.44‰ and 0.86‰ respectively (this study and Genot et al., 2020). Therefore, in urban

environments, the formation of black crusts overwhelmingly results (>90%) from the oxidation of SO_2 by O_2-TMI and H_2O_2. On the contrary, the large O-MIF measured in black crust from this study (up to 4‰) is correlated to atmospheric environments influenced by volcanic emissions, and can be explained by a large proportion (up to 44%) of SO_2 oxidized by ozone on the building walls.

4.2.2. Alteration of volcanic particles as an enhancer of the ozone oxidation

In samples from groups 2 and 3, where the $\Delta^{17}O$ is the highest, the SEM analyses show the presence of altered volcanic particles such as volcanic glass or silicates (feldspars) among gypsum and calcite minerals (Fig. 2e, 2f, 2g and 2h), which is not observed at all in samples from group 1. Alteration of volcanic glass by water is a well-studied process (Fisher & Schmincke, 1984; Friedman, 1984; Cerling et al., 1985; Stroncik & Schmincke, 2002) which tends to release mobile alkaline and alkaline earth metals such as Ca^{2+}, K^+ and Na^+ either by an interdiffusion process or ion exchange with hydrogenated species (e.g. White & Claassen, 1980). The alteration of silicate crystals such as feldspars that are Ca-Na-K-rich silicates (anorthite (R2), albite (R3) and orthoclase (R4) also leads to the release of Ca^{2+}, Na^+ and K^+ according to the following reactions (Chamley, 1989; Stumm & Wollast, 1990):

$$CaAl_2Si_2O_8 + 2CO_2 + 3H_2O = Al_2Si_2O_5(OH)_4 + Ca^{2+} + 2HCO_3^- \quad (R2)$$

$$2NaAlSi_3O_8 + 2CO_2 + 6H_2O = Al_2Si_4O_{10}(OH)_2 + 2Na^+ + 2HCO_3^- + 2H_4SiO_4 \quad (R3)$$

$$2KAlSi_3O_8 + 11H_2O = Al_2Si_2O_5(OH)_4 + 4Si(OH)_4 + 2(K,OH) \quad (R4)$$

The net result of these processes is an increase in the aqueous environment alkalinity via the release of bicarbonate (HCO_3^-) and alkaline ions. Thus, during the black crust formation, we propose that the alteration of volcanic glass and silicates particles contributes to buffer or even increase the pH of the stonewall humid layer, where the sulphate from black crust forms by SO_2 oxidation.

In atmospheric aqueous environments (droplets of water, aerosols), depending on the pH, various tropospheric oxidants are involved in the oxidation of SO_2 into sulphate. While the H_2O_2 oxidation channel is dominant for pH < 6 and leads to low $\Delta^{17}O$ values, the O_3 oxidation channel becomes dominant at pH > 6 and leads to large $\Delta^{17}O$ in the end-product sulphate (Lee & Thiemens, 2001; Martin et al., 2014; Galeazzo et al., 2018). In standard urban areas, black crust sulphates show $\Delta^{17}O$ < 1‰, which is explained by an oxidation via O_2-TMI + H_2O_2 in rather acidic conditions (pH < 6) in the humid layer on the wall surface. However, the larger $\Delta^{17}O$ (up to 4‰) measured in this study, can only be explained by a large contribution of O_3 in the SO_2 oxidation and therefore less acidic conditions. Consequently, alteration of volcanic particles in black crusts can promote the SO_2 oxidation via O_3 by increasing the pH of the humid layer where the black crust forms, rather than by a change in oxidant concentrations. More speculatively, it is also possible that volcanic particles catalysed SO_2 oxidation into sulphate, in the same way as carbonaceous particles and fly-ash do (Del Monte et al., 1981; Moropoulou et al., 1998; Ausset et al., 1999). Thus, in areas downwind an active volcano, black crust formation could be enhanced.

4.3. Outline of black crust formation mechanism

The schema in figure 8 summarises outlines of mechanisms which could be responsible for black crust formation as well as their S- and O-MIF signatures. The first possibility to form gypsum is through the acid attack of the carbonate stone wall by atmospheric sulphate aerosols (H_2SO_4 from rainwater typically). As observed in sulphate aerosols from urban areas, the resulting gypsum (referred to as Aerosol-type Gypsum; Figure 8) is expected to exhibit $\Delta^{17}O$ close to or > to 0‰ (depending on the oxidant involved in the formation of sulphate aerosols in the atmosphere; OH, O_2-TMI, H_2O_2 or O_3), $\Delta^{33}S$ > 0‰, and $\Delta^{36}S$ ranging between -1.5‰ and 1‰. Given the sulphur isotopic compositions measured in black crusts ($\Delta^{33}S$ < 0‰ and -0.5‰ < $\Delta^{36}S$ < 0.5‰), even if not totally excluded, Aerosol-type Gypsum cannot be the major component of black crusts. The second and dominant formation process of black crust gypsum is initiated by the dry deposition of SO_2 on the humid stone surface. It

sticks directly to the surface where it is dissolved in a thin liquid layer. According to the $\Delta^{33}S$ and $\Delta^{36}S$ values from this study and from Genot et al. (2020), a mass-independent fractionating process (for instance, a possible magnetic isotopic effect) must be operating during the oxidation of deposited SO_2 and conversion into calcium sulphate. In standard urban atmospheres, SO_2 is mostly oxidized into sulphate by H_2O_2 and O_2-TMI, leading to the formation of gypsum with 0‰ < $\Delta^{17}O$ < 1‰ and referred to as Urban-type Gypsum (Figure 8). In urban areas under the influence of volcanic emissions (e.g. downwind of an active volcano), the SO_2 oxidation by O_3 is highly enhanced, leading to the formation of gypsum with $\Delta^{17}O$ > 1‰ referred to as Volcanic-type Gypsum (Figure 8). Although the S- and O-multi-isotopic composition of black crust sulphates provides critical constraints on their general formation mechanism, laboratory experiments on the black crust formation could certainly help to test and refine our understanding of mechanisms, including the formation of high $\Delta^{17}O$ black crusts in the presence of volcanic particles.

Conclusion

This work extends the study of black crust isotopic compositions from the urban Parisian Basin (Genot et al., 2020) to Sicily with more variable environments (e.g. volcanic and/or marine influenced environments). The Sicilian black crusts exhibit S- and O-MIF signatures as singular as in the Paris Basin, suggesting that the formation mechanism for all black crusts worldwide is similar. Their sulphur signatures ($\Delta^{33}S$ and $\Delta^{36}S$) confirm that black crust is not formed from the deposition of atmospheric sulphate on walls but rather from dry deposition of SO_2. The black crust anionic and isotopic ($\delta^{34}S$ and $\delta^{18}O$) compositions show that, whatever the context, most of this SO_2 is of anthropogenic origin. $\Delta^{17}O$ values confirm that the SO_2 oxidation to sulphate and then gypsum on the stone wall is dominated by O_2-TMI and H_2O_2 pathways in standard rural to urban environments. It also highlights for the first time that in volcanic influenced environments, the formation of black crusts through SO_2 oxidation by ozone is enhanced. The results of the present study provide a working base for designing laboratory experiments needed to test the proposed mechanisms and elucidate

the role of volcanic particles in the enhancement of ozone oxidation in black crust formation and stone deterioration.

Acknowledgments

We are very grateful to Sorbonne University for its financial support through the “Emergence” and “Multi-disciplinary PhD Project” grants. We also thank the Agence National de la Recherche (ANR) via the contracts 14-CE33-0009-02-FOFAMIFS and 16-CE31-0010-PaleOX. We thank O. Boudouma for the SEM analyses and L. Whiteley for proofreading this manuscript. Finally, this manuscript was improved by the constructive comments from two anonymous reviewers.

References

Aiuppa, A., Bellomo, S., Brusca, L., D’Alessandro, W., Di Paola, R., & Longo, M. (2005). Major-ion bulk deposition around an active volcano (Mt. Etna, Italy). *Bulletin of Volcanology*, *68*(3), 255–265. https://doi.org/10.1007/s00445-005-0005-x

Aiuppa, A., Bonfanti, P., Brusca, L., Alessandro, W. D., Federico, C., & Parello, F. (2001). Evaluation of the environmental impact of volcanic emissions from the chemistry of rainwater : Mount Etna area (Sicily). *Applied Geochemistry*, *16*.

Alexander, B., Allman, D. J., Amos, H. M., Fairlie, T. D., Dachs, J., Hegg, D. A., & Sletten, R. S. (2012). Isotopic constraints on the formation pathways of sulfate aerosol in the marine boundary layer of the subtropical northeast Atlantic Ocean. *Journal of Geophysical Research Atmospheres*, *117*(6), 1–17. https://doi.org/10.1029/2011JD016773

Alexander, B., Park, R. J., Jacob, D. J., Li, Q. B., & Yantosca, R. M. (2005). Sulfate formation in sea-salt aerosols : Constraints from oxygen isotopes. *Journal of Geophysical Research*, *110*, 1–12. https://doi.org/10.1029/2004JD005659

Alexander, B., Savarino, J., Barkov, N. I., Delmas, R. J., & Thiemens, M. H. (2002). Climate driven changes in the oxidation pathways of atmospheric sulfur. *Geophysical Research Letters*, *29*(14), 30-1-30–34. https://doi.org/10.1029/2002gl014879

Alexander, B., Savarino, J., Kreutz, K. J., & Thiemens, M. H. (2004). Impact of preindustrial biomass-burning emissions on the oxidation pathways of tropospheric sulfur and

nitrogen. *Journal of Geophysical Research D: Atmospheres*, *109*(8), 1–8. https://doi.org/10.1029/2003JD004218

Andronico, D., & Del Carlo, P. (2016). PM10 measurements in urban settlements after lava fountain episodes at Mt. Etna, Italy: Pilot test to assess volcanic ash hazard to human health. *Natural Hazards and Earth System Sciences*, *16*(1), 29–40. https://doi.org/10.5194/nhess-16-29-2016

Andronico, D., Spinetti, C., Cristaldi, A., & Buongiorno, M. F. (2009). Observations of Mt. Etna volcanic ash plumes in 2006: An integrated approach from ground-based and polar satellite NOAA-AVHRR monitoring system. *Journal of Volcanology and Geothermal Research*, *180*(2–4), 135–147. https://doi.org/10.1016/j.jvolgeores.2008.11.013

Au Yang, D., Bardoux, G., Assayag, N., Laskar, C., Widory, D., & Cartigny, P. (2018). Atmospheric SO2oxidation by NO2plays no role in the mass independent sulfur isotope fractionation of urban aerosols. *Atmospheric Environment*, *193*(2), 109–117. https://doi.org/10.1016/j.atmosenv.2018.09.007

Au Yang, David, Cartigny, P., Desboeufs, K., Widory, D., Yang, D., Cartigny, P., … Widory, D. (2019). Seasonality in the ∆ 33 S measured in urban aerosols highlights an additional oxidation pathway for atmospheric SO 2 To cite this version : HAL Id : insu-02180508 Seasonality in the 33 S measured in urban aerosols highlights an additional oxidation pathwa.

Ausset, P., Bannery, F., Monte, M. Del, & Lefevre, R. A. (1998). Recording of pre-industrial atmospheric environment by ancient crusts on stone monuments. *Atmospheric Environment*, *32*(16), 2859–2863. https://doi.org/10.1016/S1352-2310(98)00063-6

Ausset, P., Del Monte, M., & Lefèvre, R. A. (1999). Embryonic sulphated black crusts on carbonate rocks in atmospheric simulation chamber and in the field: Role of carbonaceous fly-ash. *Atmospheric Environment*, *33*(10), 1525–1534. https://doi.org/10.1016/S1352-2310(98)00399-9

Ausset, P., & Lefevre, R. (2000). EARLY MECHANISMS OF DEVELOPMENT OF SULPHATED BLACK CRUSTS ON CARBONATE STONE. *Journal of Chemical Information and Modeling*, *53*(9), 1689–1699. https://doi.org/10.1017/CBO9781107415324.004

Bao, H. (2005). Sulfate in modern playa settings and in ash beds in hyperarid deserts: Implication for the origin of17O-anomalous sulfate in an Oligocene ash bed. *Chemical Geology*, *214*(1–2), 127–134. https://doi.org/10.1016/j.chemgeo.2004.08.052

Bao, H. (2015). Sulfate: A time capsule for Earth's O2, O3, and H2O. *Chemical Geology*, *395*, 108–118. https://doi.org/10.1016/j.chemgeo.2014.11.025

Bao, H., Cao, X., & Hayles, J. A. (2016). Triple Oxygen Isotopes: Fundamental Relationships and Applications. *Annual Review of Earth and Planetary Sciences*, *44*(1), 463–492. https://doi.org/10.1146/annurev-earth-060115-012340

Bao, H., Lyons, J. R., & Zhou, C. (2008). Triple oxygen isotope evidence for elevated CO2 levels after a Neoproterozoic glaciation. *Nature*, *453*(7194), 504–506. https://doi.org/10.1038/nature06959

Bao, H., Michalski, G., & Thiemens, M. (2001). Sulfate oxygen 17 anomalies in desert varnishes. *Geochimica et Cosmochimica Acta*, *65*(13), 2029–2036.

Bao, H., & Thiemens, M. H. (2000). Generation of O 2 from BaSO 4 Using a CO 2 −Laser Fluorination System for Simultaneous Analysis of δ 18 O and δ 17 O. *Analytical Chemistry*, *72*(17), 4029–4032. https://doi.org/10.1021/ac000086e

Bao, H., Thiemens, M. H., Farquhar, J., Campbell, D. A., Lee, C. C. W., Heine, K., & Loope, D. B. (2000). Anomalous 17O compositions in massive sulphate deposit on the earth. *Nature*, *406*(6792), 176–178. https://doi.org/10.1038/35018052

Bao, H., Thiemens, M. H., Loope, D. B., & Yuan, X. L. (2003). Sulfate oxygen-17 anomaly in an Oligocene ash bed in mid-North America: Was it the dry fogs? *Geophysical Research Letters*, *30*(16). https://doi.org/10.1029/2003GL016869

Bao, H., Yu, S., & Tong, D. Q. (2010). Massive volcanic SO2 oxidation and sulphate aerosol deposition in Cenozoic North America. *Nature*, *465*(7300), 909–912. https://doi.org/10.1038/nature09100

Barca, D., Belfiore, C. M., Crisci, G. M., La Russa, M. F., Pezzino, A., & Ruffolo, S. A. (2011). A new methodological approach for the chemical characterization of black crusts on building stones: A case study from the Catania city centre (Sicily, Italy). *Journal of Analytical Atomic Spectrometry*, *26*(5), 1000–1011. https://doi.org/10.1039/c0ja00226g

Behlen, A., Steiger, M., & Dannecker, W. (2008). Deposition of sulfur dioxide to building stones: The influence of the ambient concentration on the deposition velocity. *Environmental Geology*, *56*(3–4), 595–603. https://doi.org/10.1007/s00254-008-1414-x

Bindeman, I. N., Eiler, J. M., Wing, B. A., & Farquhar, J. (2007). Rare sulfur and triple oxygen isotope geochemistry of volcanogenic sulfate aerosols. *Geochimica et Cosmochimica Acta*, *71*(9), 2326–2343. https://doi.org/10.1016/j.gca.2007.01.026

Britton, L. G., & Clarke, A. G. (1980). Heterogeneous reactions of sulphur dioxide and SO 2 NO 2 mixtures with a carbon soot aerosol. *Atmospheric Environment (1967)*, *14*(7), 829–839. https://doi.org/10.1016/0004-6981(80)90139-0

Buchachenko, A. L. (2001). Magnetic isotope effect: Nuclear spin control of chemical reactions. *Journal of Physical Chemistry A*, *105*(44). https://doi.org/10.1021/jp011261d

Bugini, R., Tabasso, M. L., & Realini, M. (2000). Rate of formation of black crusts on marble. A case study. *Journal of Cultural Heritage*, *1*(2), 111–116. https://doi.org/10.1016/S1296-2074(00)00161-8

Buzek, F., & Šrámek, J. (1985). Sulfur isotopes in the study of stone monument conservation. *Studies in Conservation*, *30*(4), 171–176. https://doi.org/10.1179/sic.1985.30.4.171

Calabrese, S., Aiuppa, A., Allard, P., Bagnato, E., Bellomo, S., Brusca, L., … Parello, F. (2011). Atmospheric sources and sinks of volcanogenic elements in a basaltic volcano (Etna, Italy). *Geochimica et Cosmochimica Acta*, *75*(23), 7401–7425. https://doi.org/10.1016/j.gca.2011.09.040

Camuffo, D, Del Monte, M., & Sabbioni, C. (1983). Origin and growth mechanisms of the sulfated crusts on urban limestone. *Water, Air, and Soil Pollution*, *19*(c), 351–359.

Camuffo, Dario, Del Monte, M., Sabbioni, C., & Vittori, O. (1982). Wetting, deterioration and visual features of stone surfaces in an urban area. *Atmospheric Environment*, *16*(9), 2253–2259. https://doi.org/10.1016/0004-6981(82)90296-7

Cardell-Fernández, C., Vleugels, G., Torfs, K., & Van Grieken, R. (2002). The processes dominating Ca dissolution of limestone when exposed to ambient atmospheric conditions as determined by comparing dissolution models. *Environmental Geology*, *43*(1–2), 160–171. https://doi.org/10.1007/s00254-002-0640-x

Carn, S. A. (2005). Quantifying tropospheric volcanic emissions with AIRS : The 2002 eruption of Mt . Etna (Italy). *Geophysical Research Letters*, *32*(Figure 1), 1–5. https://doi.org/10.1029/2004GL021034

Cerling, T. E., Brown, F. H., & Bowman, J. R. (1985). Low-temperature alteration of volcanic glass: Hydration, Na, K, 18O and Ar mobility. *Chemical Geology: Isotope Geoscience Section*, *52*(3–4), 281–293. https://doi.org/10.1016/0168-9622(85)90040-5

Chamley, H. (1989). Clay Formation Through Weathering. *Clay Sedimentology*, 21–50. https://doi.org/10.1007/978-3-642-85916-8_2

Charola, A. E., & Ware, R. (2002). Acid deposition and the deterioration of stone: A brief review of a broad topic. *Geological Society Special Publication*, *205*, 393–406. https://doi.org/10.1144/GSL.SP.2002.205.01.28

Chen, Q., Geng, L., Schmidt, J., Xie, Z., Kang, H., Dachs, J., … Alexander, B. (2016). Isotopic constraints on the role of hypohalous acids in sulfate aerosol formation in the remote marine boundary layer. *Atmospheric Chemistry and Physics*, *16*(17), 11433–11450. https://doi.org/10.5194/acp-16-11433-2016

Cheng, Y., Zheng, G., Wei, C., Mu, Q., Zheng, B., Wang, Z., … Su, H. (2016). Reactive nitrogen chemistry in aerosol water as a source of sulfate during haze events in China. *Science Advances*, *2*(12). https://doi.org/10.1126/sciadv.1601530

Cofer, W. R., Schryer, D. R., & Rogowski, R. S. (1981). The oxidation of SO2 on carbon particles in the presence of O3, NO2 and N2O. *Atmospheric Environment (1967)*, *15*(7), 1281–1286. https://doi.org/10.1016/0004-6981(81)90321-8

Cofer, Wesley R., Schryer, D. R., & Rogowski, R. S. (1980). The enhanced oxidation of SO2 by NO2 on carbon particulates. *Atmospheric Environment (1967)*, *14*(5), 571–575. https://doi.org/10.1016/0004-6981(80)90028-8

Comite, V., Álvarez de Buergo, M., Barca, D., Belfiore, C. M., Bonazza, A., La Russa, M. F., … Ruffolo, S. A. (2017). Damage monitoring on carbonate stones: Field exposure tests contributing to pollution impact evaluation in two Italian sites. *Construction and Building Materials*, *152*, 907–922. https://doi.org/10.1016/j.conbuildmat.2017.07.048

Comite, Valeria, & Fermo, P. (2018). The effects of air pollution on cultural heritage: The case study of Santa Maria delle Grazie al Naviglio Grande (Milan)⋆. *European Physical Journal Plus*, *133*(12). https://doi.org/10.1140/epjp/i2018-12365-6

Corvo, F., Reyes, J., Valdes, C., Villaseñor, F., Cuesta, O., Aguilar, D., & Quintana, P. (2010). Influence of air pollution and humidity on limestone materials degradation in historical buildings located in cities under tropical coastal climates. *Water, Air, and Soil Pollution*, *205*(1–4), 359–375. https://doi.org/10.1007/s11270-009-0081-1

Davis, B. L. (1981). Quantitative analysis of crystalline and amorphous airborne particulates in the Provo-orem vicinity, Utah. *Atmospheric Environment*, *15*(4), 613–618. https://doi.org/10.1016/0004-6981(81)90192-X

De Hoog, J. C. M., Taylor, B. E., & Van Bergen, M. J. (2001). Sulfur isotope systematics of basaltic lavas from Indonesia: Implications for the sulfur cycle in subduction zones. *Earth and Planetary Science Letters*, *189*(3–4), 237–252. https://doi.org/10.1016/S0012-

821X(01)00355-7

Defouilloy, C., Cartigny, P., Assayag, N., Moynier, F., & Barrat, J. A. (2016). High-precision sulfur isotope composition of enstatite meteorites and implications of the formation and evolution of their parent bodies. *Geochimica et Cosmochimica Acta*, *172*, 393–409. https://doi.org/10.1016/j.gca.2015.10.009

Del Monte, M, Sabbioni, C., & Vittori, O. (1981). Airborne Carbon Particles Deterioration. *Atmospheric Environment*.

Del Monte, Marco, Ausset, P., Lefèvre, R. A., & Thiébault, S. (2001). Evidence of pre-industrial air pollution from the Heads of the Kings of Juda statues from Notre Dame Cathedral in Paris. *Science of the Total Environment*, *273*(1–3), 101–109. https://doi.org/10.1016/S0048-9697(00)00847-0

Eiler, J. M. (2001). Oxygen Isotope Variations of Basaltic Lavas and Upper Mantle Rocks, 319–364.

Farkas, O., Siegesmund, S., Licha, T., & Török, Á. (2018). Geochemical and mineralogical composition of black weathering crusts on limestones from seven different European countries. *Environmental Earth Sciences*, *77*(5). https://doi.org/10.1007/s12665-018-7384-8

Farquhar, J., Bao, H., & Thiemens, M. (2000). Atmospheric influence of Earth's earliest sulfur cycle. *Science*, *289*(5480), 756–758. https://doi.org/10.1126/science.289.5480.756

Farquhar, James, Johnston, D. T., & Wing, B. A. (2007). Implications of conservation of mass effects on mass dependent isotope fractionations: Influence of network structure on sulfur isotope phase space of dissimilatory sulfate reduction. *Geochimica et Cosmochimica Acta*, *71*(24), 5862–5875. https://doi.org/10.1016/j.gca.2007.08.028

Farquhar, James, Thiemens, M. H., & Savarino, J. (2001). Observation of wavelenght-sensitive mass-independent sulfur isotope effects during SO2 photolysis: Implications for the early atmosphere. *Journal of Geophysical Research : Atmospheres*, *106*(2000), 32829–32839.

Farquhar, James, & Wing, B. A. (2003). Multiple sulfur isotopes and the evolution of the atmosphere. *Earth and Planetary Science Letters*, *213*, 1–13. https://doi.org/10.1016/S0012-821X(03)00296-6

Fisher, R. V., & Schmincke, H.-U. (1984). Chapter 12 - Alteration of Volcanic glass. *Pyroclastic Rocks*, (3), 472.

Friedman, I. (1984). Volcanic glasses, their origins and alteration processes. *Journal of Non-Crystalline Solids*, *67*, 127–133.

Fronteau, G., Schneider-thomachot, C., Chopin, E., Barbin, V., Mouze, D., & Garros, R. (2010). Black-crust growth and interaction with underlying limestone microfacies. *Natural Stone Resources for Historical Monuments*, 25–34.

Galeazzo, T., Bekki, S., Martin, E., Savarino, J., Arnold, S. R., & Ipsl, L. (2018). Photochemical box modelling of volcanic SO 2 oxidation : isotopic constraints. *Atmospheric Chemistry and Physics*, 17909–17931.

Gautier, E., Savarino, J., Hoek, J., Erbland, J., Caillon, N., Hattori, S., … Farquhar, J. (2019). 2600-Years of Stratospheric Volcanism Through Sulfate Isotopes. *Nature Communications*, *10*(1), 1–7. https://doi.org/10.1038/s41467-019-08357-0

Genot, I., Yang, D. A., Martin, E., Cartigny, P., Legendre, E., & De, M. (2020). Oxygen and sulfur mass-independent isotopic signatures in black crusts : the complementary negative Δ 33 S-reservoir of sulfate aerosols ? *Atmospheric Chemistry and Physics*, *40*(October), 1–31.

Guerrieri, L., Merucci, L., Corradini, S., & Pugnaghi, S. (2015). Evolution of the 2011 Mt. Etna ash and SO2 lava fountain episodes using SEVIRI data and VPR retrieval approach. *Journal of Volcanology and Geothermal Research*, *291*, 63–71. https://doi.org/10.1016/j.jvolgeores.2014.12.016

Guo, Z., Li, Z., Farquhar, J., Kaufman, A. J., Wu, N., Li, C., … Wang, P. (2010). Identification of sources and formation processes of atmospheric sulfate by sulfur isotope and scanning electron microscope measurements. *Journal of Geophysical Research*, *115*, 1–13. https://doi.org/10.1029/2009jd012893

Han, X., Guo, Q., Strauss, H., Liu, C., Hu, J., Guo, Z., … Kong, J. (2017). Multiple sulfur isotope constraints on sources and formation processes of sulfate in Beijing PM2 . 5 aerosol. *Environmental Science and Technology*.

Haneef, S. J., Johnson, J. B., Dickinson, C., Thompson, G. E., & Wood, G. C. (1992). Effect of dry deposition of NOx and SO2 gaseous pollutants on the degradation of calcareous building stones. *Atmospheric Environment Part A, General Topics*, *26*(16), 2963–2974. https://doi.org/10.1016/0960-1686(92)90288-V

Harris, E., Sinha, B., Foley, S., Crowley, J. N., Borrmann, S., & Hoppe, P. (2012). Sulfur isotope fractionation during heterogeneous oxidation of SO2 on mineral dust. *Atmospheric Chemistry and Physics*, *12*(11), 4867–4884. https://doi.org/10.5194/acp-

12-4867-2012

Harris, E., Sinha, B., Hoppe, P., Crowley, J. N., Ono, S., & Foley, S. (2012). Sulfur isotope fractionation during oxidation of sulfur dioxide: Gas-phase oxidation by OH radicals and aqueous oxidation by H2O2, O3 and iron catalysis. *Atmospheric Chemistry and Physics*, *12*(1), 407–424. https://doi.org/10.5194/acp-12-407-2012

Harris, Eliza, Sinha, B., Hoppe, P., & Ono, S. (2013). High-precision measurements of 33S and 34S fractionation during SO2 oxidation reveal causes of seasonality in SO2 and sulfate isotopic composition. *Environmental Science and Technology*, *47*(21), 12174–12183. https://doi.org/10.1021/es402824c

Harris, Eliza, Sinha, B., Van Pinxteren, D., Tilgner, A., Fomba, K. W., Schneider, J., … Herrmann, H. (2013). Enhanced role of transition metal ion catalysis during in-cloud oxidation of SO2. *Science*, *340*(6133), 727–730. https://doi.org/10.1126/science.1230911

Holt, B. D., & Kumar, R. (1991). *Oxygen Isotope Fractionation for Understanding the Sulphur Cycle*.

Holynska, B., Gilewicz-Wolter, J., Ostachowicz, B., Bielewski, M., Streli, C., & Wobrauschek, P. (2004). Study of the deterioration of sandstone due to acid rain and humid so 2 gas. *X-Ray Spectrometry*, *33*(5), 342–348. https://doi.org/10.1002/xrs.723

Jenkins, Kathryn, & Bao. (2006). Multiple oxygen and sulfur isotope compositions of atmospheric sulfate in Baton Rouge , LA , USA. *Atmospheric Environment*, *40*, 4528–4537. https://doi.org/10.1016/j.atmosenv.2006.04.010

Klemm, W., & Siedel, H. (2002). Evaluation of the origin of sulphate compounds in building stone by sulphur isotope ratio. *Geological Society Special Publication*, *205*, 419–429. https://doi.org/10.1144/GSL.SP.2002.205.01.30

Kloppmann, W., Bromblet, P., Vallet, J. M., Vergès-Belmin, V., Rolland, O., Guerrot, C., & Gosselin, C. (2011). Building materials as intrinsic sources of sulphate: A hidden face of salt weathering of historical monuments investigated through multi-isotope tracing (B, O, S). *Science of the Total Environment*, *409*(9), 1658–1669. https://doi.org/10.1016/j.scitotenv.2011.01.008

Kramar, S., Mirtič, B., Knöller, K., & Rogan-Šmuc, N. (2011). Weathering of the black limestone of historical monuments (Ljubljana, Slovenia): Oxygen and sulfur isotope composition of sulfate salts. *Applied Geochemistry*, *26*(9–10), 1632–1638. https://doi.org/10.1016/j.apgeochem.2011.04.020

La Russa, M. F., Comite, V., Aly, N., Barca, D., Fermo, P., Rovella, N., … Ruffolo, S. A. (2018). Black crusts on Venetian built heritage, investigation on the impact of pollution sources on their composition. *European Physical Journal Plus*, *133*(9). https://doi.org/10.1140/epjp/i2018-12230-8

La Russa, M. F., Fermo, P., Comite, V., Belfiore, C. M., Barca, D., Cerioni, A., … Ruffolo, S. A. (2017). The Oceanus statue of the Fontana di Trevi (Rome): The analysis of black crust as a tool to investigate the urban air pollution and its impact on the stone degradation. *Science of the Total Environment*, *593–594*, 297–309. https://doi.org/10.1016/j.scitotenv.2017.03.185

Labidi, J., Cartigny, P., Birck, J. L., Assayag, N., & Bourrand, J. J. (2012). Determination of multiple sulfur isotopes in glasses: A reappraisal of the MORB δ34S. *Chemical Geology*, *334*, 189–198. https://doi.org/10.1016/j.chemgeo.2012.10.028

Lanzafame, R., Scandura, P. F., Famoso, F., Monforte, P., & Oliveri, C. (2014). Air quality data for Catania: Analysis and investigation case study 2010-2011. *Energy Procedia*, *45*(2), 681–690. https://doi.org/10.1016/j.egypro.2014.01.073

Le Gendre, E., Martin, E., Villemant, B., Cartigny, P., & Assayag, N. (2016). A simple and reliable anion-exchange resin method for sulfate extraction and purification suitable for multiple O- and S-isotope measurements. *Communication in Mass Spectrometry*, (October 2016), 137–144. https://doi.org/10.1002/rcm.7771

Lee, Savarino, T. (2001). Mass Independent O Isotopic Composition of atmospheric sulfate : origin and implications for the present and past atmosphere of Earth and Mars. *Geophysical Research Letters*.

Lee, C C, Savarino, J., Cachier, H., Thiemens, M. H., Savarino, J., Cachier, H., & Sulfur, M. H. T. (2002). Tellus B : Chemical and Physical Meteorology Sulfur (S , S , S , S) and oxygen (O , O , O) isotopic ratios of primary sulfate produced from combustion processes. *Chemical and Physical Meteorology*, *0889*. https://doi.org/10.3402/tellusb.v54i3.16660

Lee, Charles Chi-woo, & Thiemens, M. H. (2001). The delta17O and delta18O measurements of atmospheric sulfate from a coastal and high alpine region : A mass-independent isotopic anomaly. *Journal of Geophysical Research*, *106*.

Lefèvre, R. A., & Ausset, P. (2002). Atmospheric pollution and building materials: Stone and glass. *Geological Society Special Publication*, *205*, 329–345. https://doi.org/10.1144/GSL.SP.2002.205.01.24

Lefèvre, R. A., Ionescu, A., Ausset, P., Chabas, A., Girardet, F., & Vince, F. (2007). Modelling of the calcareous stone sulphation in polluted atmosphere after exposure in the field. *Geological Society Special Publication*, *271*, 131–137. https://doi.org/10.1144/GSL.SP.2007.271.01.14

Lin, M., Kang, S., Shaheen, R., Li, C., Hsu, S.-C., & Thiemens, M. H. (2018). Atmospheric sulfur isotopic anomalies recorded at Mt. Everest across the Anthropocene. *Proceedings of the National Academy of Sciences*, *115*(27), 6964–6969. https://doi.org/10.1073/pnas.1801935115

Livingston, R. A. (2012). MASS BALANCE EVIDENCE FOR HYDROCHLORIC ACID VAPOR ATTACK ON THE MARBLE OF THE STATUE OF PHOENICIA BY SEA SALT DECHLORINIZATION R., (Camerman 1954), 1–9.

Longinelli, A., & Bartelloni, M. (1978). Atmospheric Pollution in Venice, Italy, as indicated by isotopic analyses, *2*, 335–341.

Martin, E, Bekki, S., Ninin, C., & Bindeman, I. (2014). Isotopic insight into volcanic sulfate formation in the troposphere. *Journal of Geophysical Research: Atmospheres*, 660–673. https://doi.org/10.1002/2014JD021915 Received

Martin, Erwan. (2018). Volcanic Plume Impact on the Atmosphere and Climate : O- and S-Isotope Insight into Sulfate Aerosol Formation. *Geosciences*, 1–23.

Martin, Erwan, & Bindeman, I. (2009). Mass-independent isotopic signatures of volcanic sulfate from three supereruption ash deposits in Lake Tecopa, California. *Earth and Planetary Science Letters*. https://doi.org/10.1016/j.epsl.2009.03.005

Massey, S. W. (1999). The effects of ozone and NO(x) on the deterioration of calcareous stone. *Science of the Total Environment*, *227*(2–3), 109–121. https://doi.org/10.1016/S0048-9697(98)00409-4

Mather, T. A., Mccabe, J. R., Rai, V. K., Thiemens, M. H., Pyle, D. M., Heaton, T. H. E., … Fern, G. R. (2006). Oxygen and sulfur isotopic composition of volcanic sulfate aerosol at the point of emission. *Journal of Geophysical Research*, *111*(May), 1–9. https://doi.org/10.1029/2005JD006584

Michalski, G., Bhattacharya, S. K., & Girsch, G. (2013). NO x cycle and tropospheric ozone isotope anomaly: an experimental investigation . *Atmospheric Chemistry and Physics Discussions*, *13*(4), 9443–9483. https://doi.org/10.5194/acpd-13-9443-2013

Monks, P. S., Archibald, A. T., Colette, A., Cooper, O., Coyle, M., Derwent, R., … Williams, M. L. (2015). Tropospheric ozone and its precursors from the urban to the global scale

from air quality to short-lived climate forcer. *Atmospheric Chemistry and Physics*, *15*(15), 8889–8973. https://doi.org/10.5194/acp-15-8889-2015

Montana, G., Randazzo, L., & Mazzoleni, P. (2012). Natural and anthropogenic sources of total suspended particulate and their contribution to the formation of black crusts on building stone materials of Catania (Sicily). *Environmental Earth Sciences*, *67*(4), 1097–1110. https://doi.org/10.1007/s12665-012-1554-x

Montana, G., Randazzo, L., Oddo, I. A., & Valenza, M. (2008). The growth of “black crusts” on calcareous building stones in Palermo (Sicily): A first appraisal of anthropogenic and natural sulphur sources. *Environmental Geology*, *56*(2), 367–380. https://doi.org/10.1007/s00254-007-1175-y

Morin, S., Sander, R., & Savarino, J. (2011). and Physics Simulation of the diurnal variations of the oxygen isotope anomaly (17 O) of reactive atmospheric species. *Atmospheric Chemistry and Physics*, 3653–3671. https://doi.org/10.5194/acp-11-3653-2011

Moropoulou, A., Bisbikou, K., Torfs, K., Van Grieken, R., Zezza, F., & MacRi, F. (1998). Origin and growth of weathering crusts on ancient marbles in industrial atmosphere. *Atmospheric Environment*, *32*(6), 967–982. https://doi.org/10.1016/S1352-2310(97)00129-5

Novakov, T., Chang, S. ., & Harker, A. . (1973). Sulfates as pollution particulates : catalytic formation on carbon (soot) particles. *Science*, *346*, 259–261.

Pozo-Antonio, J. S., Pereira, M. F. C., & Rocha, C. S. A. (2017). Microscopic characterisation of black crusts on different substrates. *Science of the Total Environment*, *584–585*, 291–306. https://doi.org/10.1016/j.scitotenv.2016.12.080

Přikryl, R., Svobodová, J., Zák, K., & Hradil, D. (2004). Anthropogenic origin of salt crusts on sandstone sculptures of Prague’s Charles Bridge (Czech Republic): Evidence of mineralogy and stable isotope geochemistry. *European Journal of Mineralogy*, *16*(4), 609–618. https://doi.org/10.1127/0935-1221/2004/0016-0609

Pye, K., & Schiavon, N. (1989). Cause of sulphate attack on concrete, render and stone indicated by sulphur isotope ratios. *Nature*, *342*(6250), 663–664. https://doi.org/10.1038/342663a0

Rees, C. E. (1970). The sulphur isotope balance of the ocean : an improved model. *Earth and Planetary Science Letters*, *7*, 366–370.

Rees C. E., Jenkins, W. J., & Monster, J. (1978). The sulphur isotopic composition. *Geochimxa et Cosmochimica Acta*, *42*(65), 377–381.

Rennie, V. C. F., & Turchyn, A. V. (2014). The preservation of δSSO434 and δOSO418 in carbonate-associated sulfate during marine diagenesis: A 25 Myr test case using marine sediments. *Earth and Planetary Science Letters*, *395*, 13–23. https://doi.org/10.1016/j.epsl.2014.03.025

Roekens, E., & van Grieken, R. (1989). Rates of air pollution induced surface recession and material loss for a cathedral in belgium. *Atmospheric Environment (1967)*, *23*(1), 271–277. https://doi.org/10.1016/0004-6981(89)90119-4

Romero, A. B., & Thiemens, M. H. (2003). Mass-independent sulfur isotopic compositions in present-day sulfate aerosols. *J. Geophys. Res.*, *108*(D16), 4524. https://doi.org/10.1029/2003JD003660

Ruffolo, S. A., Comite, V., La Russa, M. F., Belfiore, C. M., Barca, D., Bonazza, A., … Sabbioni, C. (2015). An analysis of the black crusts from the Seville Cathedral: A challenge to deepen the understanding of the relationships among microstructure, microchemical features and pollution sources. *Science of the Total Environment*, *502*, 157–166. https://doi.org/10.1016/j.scitotenv.2014.09.023

Sabbioni, C. (1995). Contribution of atmospheric deposition to the formation of damage layers. *Science of the Total Environment*, *167*(1–3), 49–55. https://doi.org/10.1016/0048-9697(95)04568-L

Savarino, J., Lee, C. C. W., & Thiemens, M. H. (2000). Laboratory oxygen isotopic study of sulfur (IV) oxidation: Origin of the mass-independent oxygen isotopic anomaly in atmospheric sulfates and sulfate mineral deposits on Earth. *Journal of Geophysical Research*, *105*.

Scollo, S., Prestifilippo, M., Spata, G., D'Agostino, M., & Coltelli, M. (2009). Monitoring and forecasting Etna volcanic plumes. *Natural Hazards and Earth System Science*, *9*(5), 1573–1585. https://doi.org/10.5194/nhess-9-1573-2009

Shaheen, R., Abauanza, M., Jackson, T. L., McCabe, J., Savarino, J., & Thiemens, M. H. (2013). Tales of volcanoes and El-Niño southern oscillations with the oxygen isotope anomaly of sulfate aerosol. *Proceedings of the National Academy of Sciences of the United States of America*, *110*(44), 17662–17667. https://doi.org/10.1073/pnas.1213149110

Shaheen, R., Abaunza, M. M., Jackson, T. L., McCabe, J., Savarino, J., & Thiemens, M. H. (2014). Large sulfur-isotope anomaly in nonvolcanic sulfate aerosol and its implications for the Archean atmosphere. *Proceedings of the National Academy of Sciences of the*

United States of America, *111*(33), 11979–11983. https://doi.org/10.1073/pnas.1406315111

Siedel, H. (2000). Evaluation of the Environmental Influence of Transport. *Proceedings of the 9th International Congress on Deterioration and Conservation of Stone*, *2*(2), 61–73. https://doi.org/10.12709/mest.02.02.02.07

Smith, J. W. (1974). The distribution and isotopic composition oi sulfur in coal. *Geochemica and Cosmochemica Acta*, *38*(1964), 121–133.

Sofen, E. D., Alexander, B., & Kunasek, S. A. (2011). The impact of anthropogenic emissions on atmospheric sulfate production pathways, oxidants, and ice core Δ17O(SO42-). *Atmospheric Chemistry and Physics*, *11*(7), 3565–3578. https://doi.org/10.5194/acp-11-3565-2011

Stroncik, N. A., & Schmincke, H. U. (2002). Palagonite – A review. *International Journal of Earth Sciences*, *91*(4), 680–697. https://doi.org/10.1007/s00531-001-0238-7

Stumm, W., & Wollast, R. (1990). Coordination chemistry of weathering: Kinetics of the surface-controlled dissolution of oxide minerals. *Reviews of Geophysics*, *28*(1), 53–69. https://doi.org/10.1029/RG028i001p00053

Thode, H. G., Monster, J., & Dunford, H. B. (1961). Sulphur isotope geochemistry. *Geochimica et Cosmochimica Acta*, *25*(3), 159–174. https://doi.org/10.1016/0016-7037(61)90074-6

Torfs, K. M., Van Grieken, R. E., & Buzek, F. (1997). Use of stable isotope measurements to evaluate the origin of sulfur in gypsum layers on limestone buildings. *Environmental Science and Technology*, *31*(9), 2650–2655. https://doi.org/10.1021/es970067v

Török, A., Tobias, L., Klaus, S., & Siegesmund, S. (2010). Urban and rural limestone weathering ; the contribution of dust to black crust formation. *Environmental Earth Sciences*, 675–693. https://doi.org/10.1007/s12665-010-0737-6

Turchyn, A. V., Schrag, D. P., Coccioni, R., & Montanari, A. (2009). Stable isotope analysis of the Cretaceous sulfur cycle. *Earth and Planetary Science Letters*, *285*(1–2), 115–123. https://doi.org/10.1016/j.epsl.2009.06.002

Vallet, J. M., Gosselin, C., Bromblet, P., Rolland, O., Vergès-Belmin, V., & Kloppmann, W. (2006). Origin of salts in stone monument degradation using sulphur and oxygen isotopes: First results of the Bourges cathedral (France). *Journal of Geochemical Exploration*, *88*(1-3 SPEC. ISS.), 358–362. https://doi.org/10.1016/j.gexplo.2005.08.075

Varrica, D., Tamburo, E., Vultaggio, M., & Di Carlo, I. (2019). ATR–FTIR spectral analysis and soluble components of PM10 and PM2.5 particulate matter over the urban area of palermo (Italy) during normal days and saharan events. *International Journal of Environmental Research and Public Health*, *16*(14). https://doi.org/10.3390/ijerph16142507

White, A. F., & Claassen, H. C. (1980). Kinetic model for the short-term dissolution of a rhyolitic glass. *Chemical Geology*, *28*(C), 91–109. https://doi.org/10.1016/0009-2541(80)90038-8

Wiese, U., Behlen, A., & Steiger, M. (2013). The influence of relative humidity on the SO2 deposition velocity to building stones: A chamber study at very low SO2 concentration. *Environmental Earth Sciences*, *69*(4), 1125–1134. https://doi.org/10.1007/s12665-012-1872-z

Wlnkler, E. M. (1966). Important agents of weathering for building and monumental stone. *Engineering Geology*, *1*(5), 381–400.

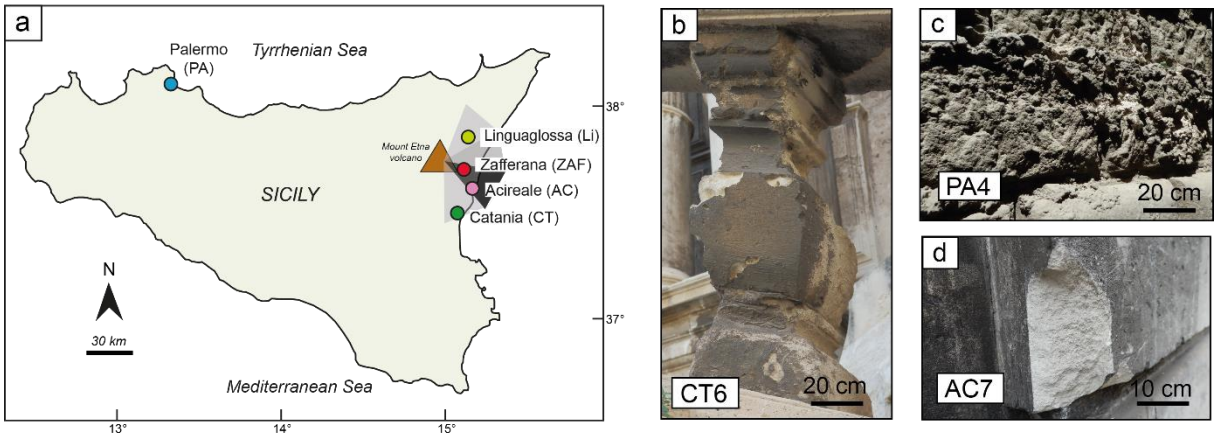

Figure *1* : a) Simplified map of Sicily showing the different sample locations : Palermo (PA) samples in blue circle, Catania (CT) samples in dark green circle, Acireale (AC) samples in pink circle, Zafferana (ZAF) samples in red circle and Linguaglossa (Li) samples in light green circle. The brown triangle corresponds to the Etna volcano. The main wind directions from the Mt Etna towards the SE are indicated: the grey zone illustrates the sporadic wind directions that can lead the volcanic emissions away towards Catania and Linguaglossa and the black zone indicates the dominant wind directions that lead the volcanic emissions away towards Zafferana and Acireale. Photos b), c), d) illustrate black crusts on highly porous carbonate stones (calcarenites of different geological age and grain-size distribution) from some of the considered sampling sites (see Table 1).

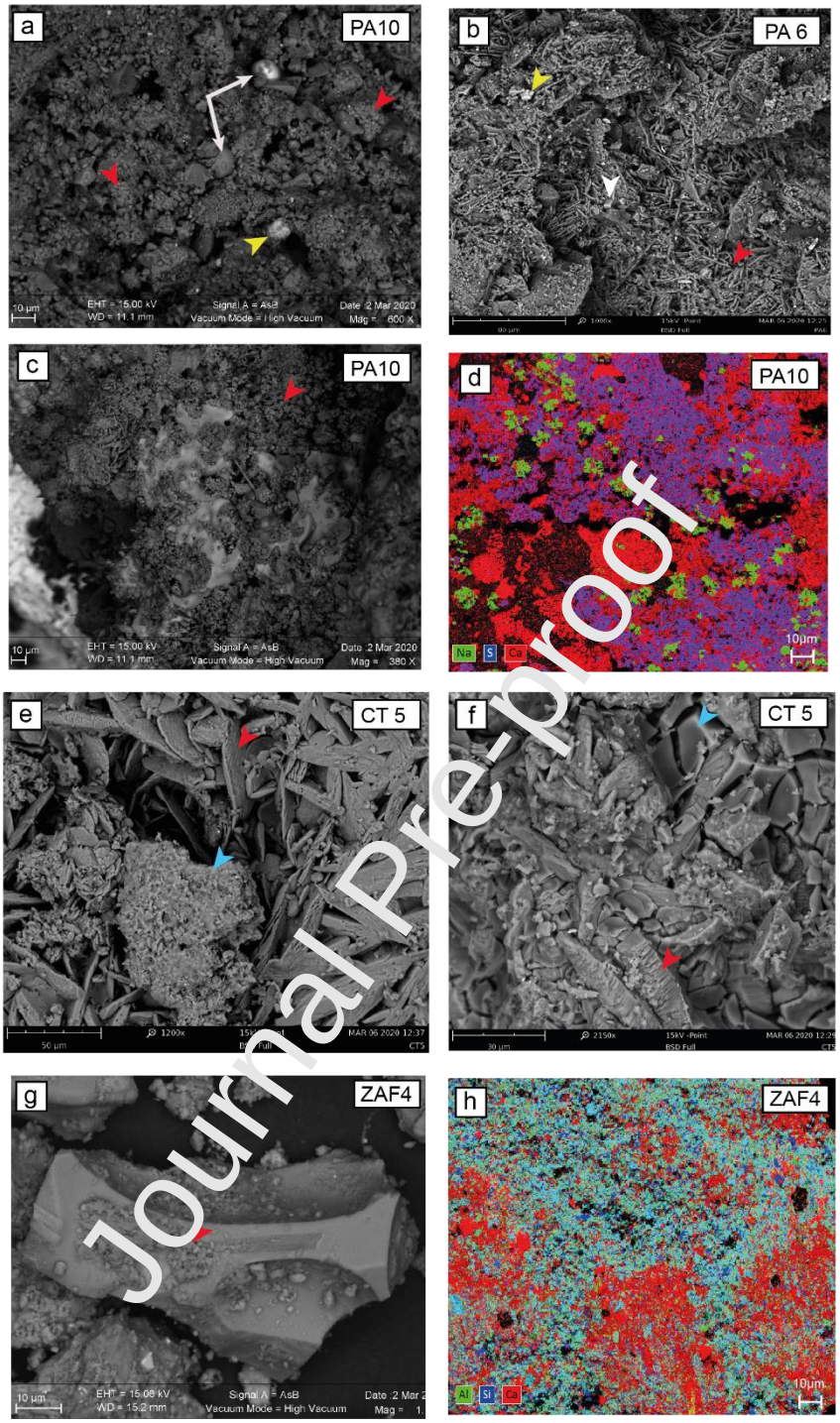

Figure 2: SEM images of black crusts from Palermo (PA-6 and PA-10) and the Etnean area (CT-5 and ZAF4). Gypsum crystals, rose-like gypsum aggregates and more chaotic gypsum aggregates are found in all samples (red arrows). Halite crystals and salt precipitation are frequently developed on black crusts from Palermo (white arrow on b, white areas on c, and green areas on d). Spherical metallic particles (white arrows on a), iron oxide (yellow arrow on a and b) are also observed in all samples. Altered volcanic glass (g) and silicates (blue arrows on e and f) are observed in black crust sampled near the Etna. d) corresponds to a chemical map showing the repartition of different major elements: Al, S and Ca. Purple zones highlight the areas with Ca and S, which correspond to gypsum and the green zones correspond to halite crystals (NaCl). f) Map showing the presence of Al, Si and Ca in black crust sampled near the Etna. Blue areas correspond to silicate particles (mineral or glass) and most of the red areas correspond to gypsum crystals.

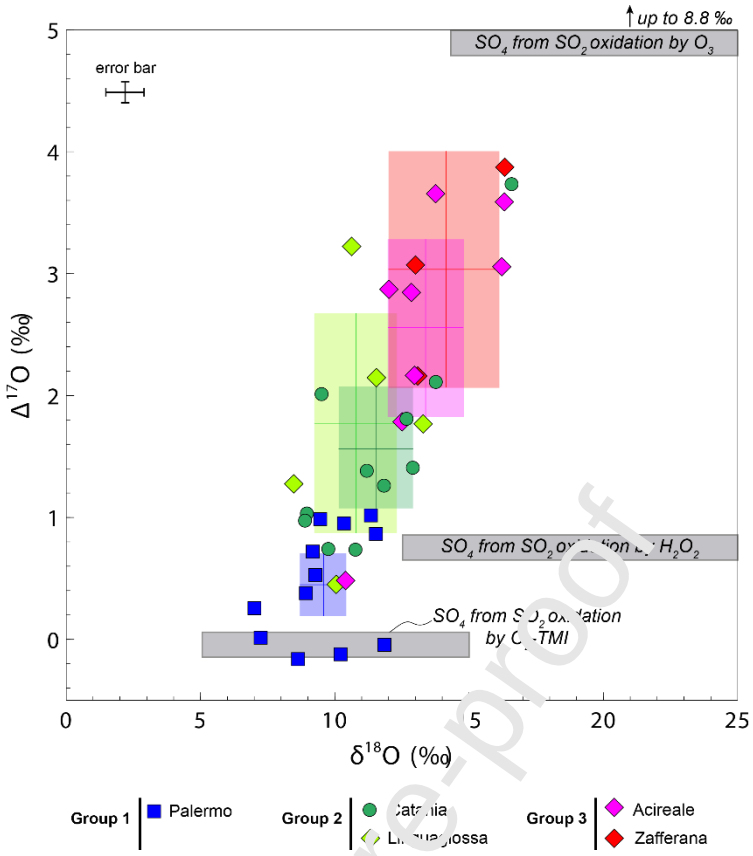

Figure 3: $\Delta^{17}O$ plotted against $\delta^{18}O$ measured in black crust sulphates from Palermo, Catania, Linguaglossa, Acireale and Zafferana. Each cross and the associated coloured area represent the average $\Delta^{17}O$ and $\delta^{18}O$ values and its standard deviation (2σ). The grey boxes represent the expected isotopic signatures of sulphate formed by O_2-TMI, H_2O_2 or O_3 oxidation pathways that are the three main oxidation channels proposed to explain our results (Savarino et al., 2000).

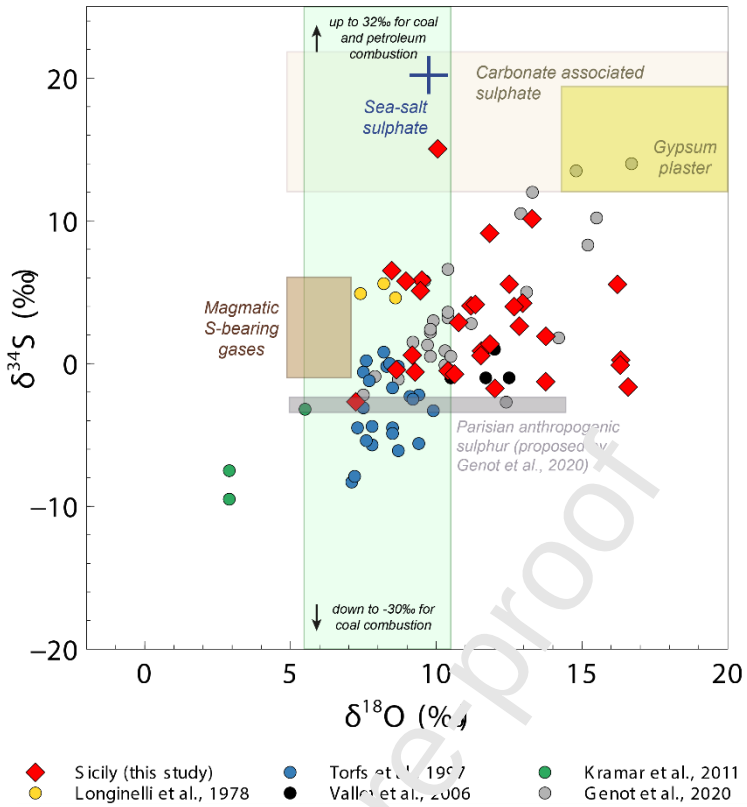

Figure 4: $\delta^{34}S$ as a function of $\delta^{18}O$ measured in sulphate from black crust from different studies. Expected values for magmatic S-bearing gases (dark brown area), modern seawater (purple cross), sea-salt sulphate (blue cross), carbonate associated sulphate (light brown), gypsum plaster (yellow area) and anthropogenic sulphur from fuel combustion (green area) are also represented. Values are taken from (De Hoog et al., 2001; Eiler, 2001; Labidi et al., 2012) for magmatic sulphur gases, from (Rees, 1970; Smith & Batts, 1974; Faure, 1986) for sulphur from fuel combustion, from (Holt & Kumar, 1991; Rees et al., 1978; Faure, 1986) for modern seawater sulphate and sea-salt sulphate, from (Turchyn et al., 2009; Rennie & Turchyn, 2014) for CAS and from (Kloppmann et al., 2011) for gypsum plaster. The grey area represents the sulphur isotopic composition of the anthropogenic end-member proposed by Genot et al., 2020.

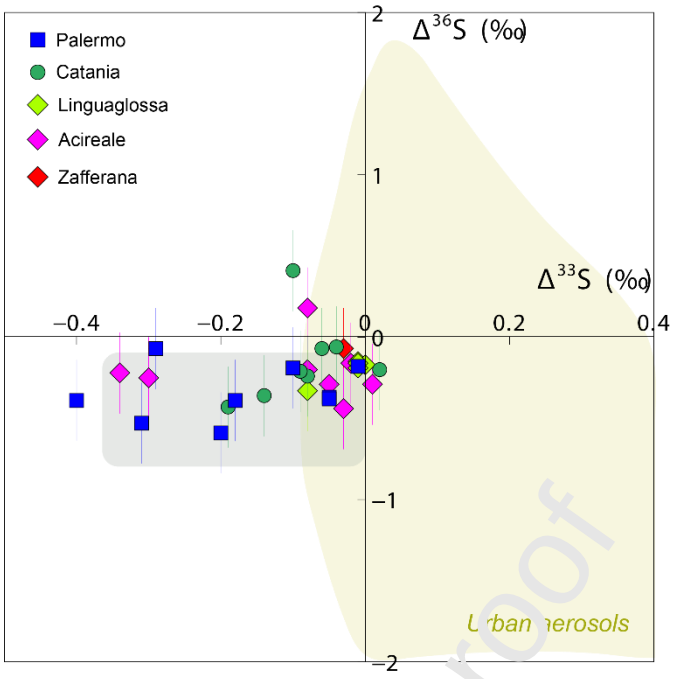

Figure 5: $\Delta^{36}S$ plotted against $\Delta^{33}S$ measured in black crust sulphates from different sites in Sicily. The grey area represents the range of $\Delta^{36}S$ and $\Delta^{33}S$ values of black crust sulphates from the Parisian Basin and the light yellow area represents the range of $\Delta^{36}S$ and $\Delta^{33}S$ values of sulphate from urban aerosols (Genot et al., 2020 and references therein).

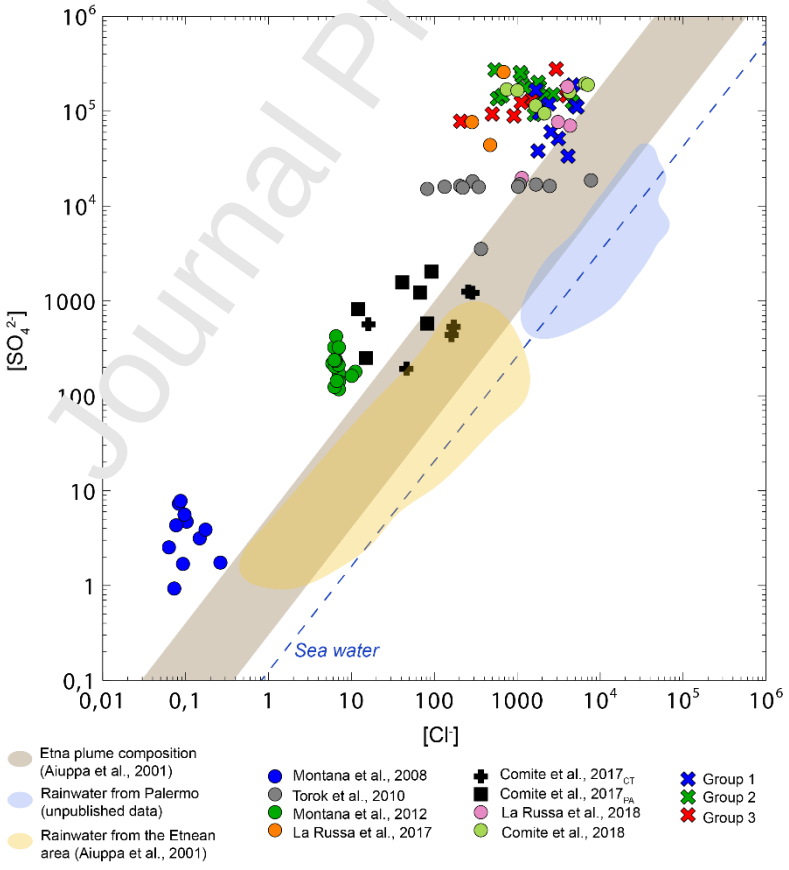

Figure 6: $[SO_4^{2-}]$ as a function of $[Cl^-]$ measured in black crusts from different studies (see legend for details). Group 1, Group 2, and Group 3 correspond to black crusts from this study. Ratios measured in seawater, in rainwaters from the Etnean area, from Palermo and in the plume of the Mt Etna are also represented (Aiuppa et al., 2001; Montana et al., 2012). It is important to notice that, since we report our concentrations to the mass of

black crust leached and that some of the other studies report concentrations from the ion chromatography measurements, the absolute concentrations between different studies are not comparable but only the $[SO_4^{2-}]/[Cl^-]$ ratios are.

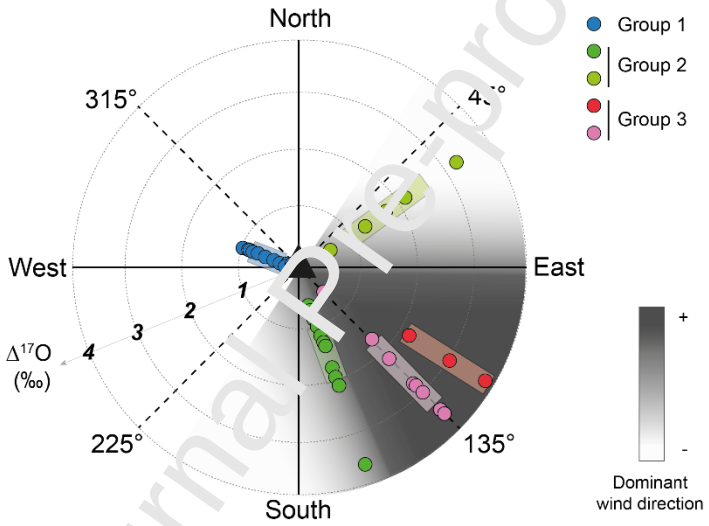

Figure 7: Wind rose representing the dominant wind direction (the darker the area is, the more prevalent the wind direction is). The measured $\Delta^{17}O$ values for each group are given by the distance to the circle centre, the rectangle represents the average value with the incertitude for each location. The dark triangle represents the Etna volcano. The darkest area (dominant wind direction) highlights the sites the most affected by volcanic emissions. It is worth noting that black crust $\Delta^{17}O$ is higher in locations under strongest influence of volcanic emission (Group 3).

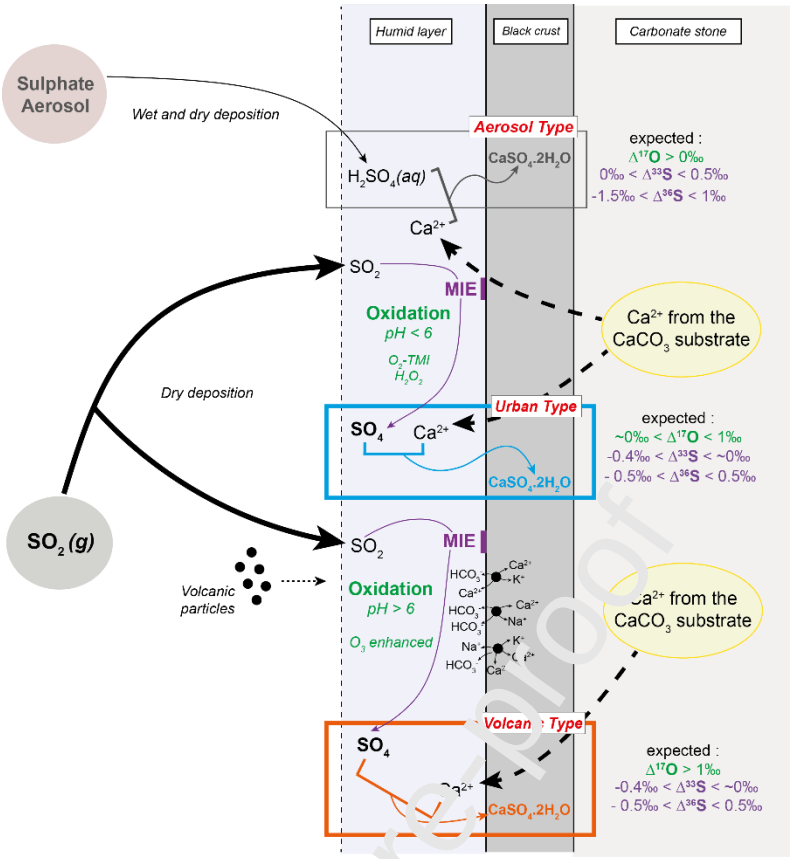

Figure 8: Schematic of possible black crust formation mechanisms. The two possible sulphur precursors for black crust formation are presented on the left-hand side. The middle part describes the possible mechanisms operating at the carbonate stone surface and the right-hand side shows the expected S- and O-MIF isotopic anomalies. SO_2 from different sources (marine, anthropogenic or volcanic) either undergo oxidation in the atmosphere to form sulphate aerosols (rainwater sulphate is included) that can be then deposited on the wet wall or SO_2 undergoes dry deposition on the wet wall. This leads to two possible mechanisms of gypsum formation via 1/ the reaction between deposited sulphuric acid and calcium from the carbonate stone, resulting in the Aerosol Type Gypsum but certainly a minor formation process according to black crust isotopic composition (black rectangle at the top); and 2/ the reaction between sulphate formed by the oxidation of deposited SO_2 on the wet stone surface and calcium from the carbonate stone substrate, which appears to be the dominant gypsum formation process according to black crust isotopic composition, resulting in Urban Type Gypsum (blue rectangle) or Volcanic Type Gypsum (orange rectangle) depending on the volcanic influence. MIE (magnetic isotope effect) proposed by Genot et al. (2020) occurs on the wet wall and is not relevant in the case of the reaction between deposited sulphuric acid and calcium from the carbonate stone (black rectangle). See section 4.3 for more details.

Table *1* : List of black crust samples with their precise location and the nature of the stone substrate. Sample names reflect their main area: PA for Palermo, CT for Catania, Li for Linguaglossa, AC for Acireale, ZAF for Zafferana and SV for Santa Venerina. (Note that in this paper, SV samples are considered as ZAF samples due to their proximity to Zafferana).

Samples	Location	Stone substrate	Type of building
PA1	Via Garibaldi 53 cross with Via Schiavuzzo	lime based mortar	private building
PA2	Via Garibaldi 59	biocalcarenite	private building
PA3	Via Alloro 123 cross with Via dei Credenzieri	reddish biocalcarenite and yellowish biocalcarenite	private building
PA4	Via Paternostro A. 40 cross Via Caltabellotta	lime mortar on biocalcarenite	Cattolica Palace
PA5	Corso Vittorio Emanuele 111	biocalcarenite	Amari Palace
PA6	Corso Vittorio Emanuele	limestone	Chiesa di Santa Maria di Portosalvo
PA7	Corso Vittorio Emanuele 39	lime based mortar	Vasallo Palace
PA8	Corso Vittorio Emanuele 31b	biocalcarenite	Chiesa di S. Maria della Catena-Archivio di Stato
PA9	Via del Celso 19	biocalcarenite	Santamarina Palace
PA10	Piazza Montevergini	biocalcarenite	Chiesa di S. Maria di Montevergini
PA11	Via del Celso 145 (in front of)	biocalcarenite	Chiesa di S. Agata alla Guilla
PA12	Piazzetta Sant'Agata alla Guilla	biocalcarenite	Chiesa di S. Agata alla Guilla
PA13	Via del Protonotaro	lime based mortar and biocalcarenite	private building
CT1	Via Auteri 52	Iblean calcarenite	private building
CT2	Via Sgroi 12	Iblean calcarenite	private building
CT3	Via Sgroi 12	basalt	private building
CT4	Via Crociferi 9	Iblean calcarenite	private building
CT5	Via Crociferi	Iblean calcarenite	Chiesa di S. Francesco Borgia - balustrade
CT6	Via Crociferi	Iblean calcarenite	Chiesa di S. Francesco Borgia - stairs
CT7	Via Crociferi	Iblean calcarenite	Chiesa di S. Francesco Borgia - right pilaster
CT8	Via S. Elena	Iblean calcarenite	Chiesa di S. Camillo-lateral facade
CT9	Via Cerami	Iblean calcarenite	Cerami Palace
CT10	Via Santa Maddalena 27	Iblean calcarenite	private building
CT11	Via Santa Maddalena 27	substrate of sample CT10	private building
CT12	Via Gesualdo Clemente	Iblean calcarenite	private building
CT13	Piazza Dante 34	substrate of sample CT14	IBAM Institute
CT14	Piazza Dante 34	Iblean calcarenite	IBAM Institute
CT15	inside of the Monastero dei Benedettini	Iblean calcarenite	Monastero dei Benedettini
CT16	Piazza Dante cross with Via Teatro Greco	basalt	Conservatorio delle Verginelle di S. Agata - Lateral facade
CT17	Via Teatro Greco 84	basalt	Conservatorio delle Verginelle di S. Agata - Lateral facade
CT18	Via Teatro Greco 84	efflorescences on basalt	Conservatorio delle Verginelle di S. Agata - Lateral facade
CT19	Via Teatro Greco 84	efflorescences on Iblean calcarenite	Conservatorio delle Verginelle di S. Agata - Lateral facade
CT20	Via Vittorio Emanuele 300	Iblean calcarenite	Valdisavoja Palace

LI1	Linguaglossa, via Camillo Benso Conte di Cavour, 21	Iblean calcarenite/plaster	private building
LI2	Linguaglossa, via Camillo Benso Conte di Cavour, 19	Iblean calcarenite	private building
LI3	Linguaglossa, via Roma 142-144	Iblean calcarenite/lime-based plaster	private building
LI4	Linguaglossa, via Roma 95-97	Iblean calcarenite	private building
LI5	Linguaglossa, via Roma 117	Iblean calcarenite	private building
ZAF1	Zafferana Etnea, Umberto I Place 24	Iblean calcarenite	private building
ZAF2	Zafferana Etnea, Via Roma 321	Iblean calcarenite/lime-based plaster	private building
ZAF3	Zafferana Etnea, Via Roma 274	Iblean calcarenite	private building
ZAF4	Zafferana Etnea, Via Roma 156	Iblean calcarenite	private building
SV1	Santa Venerina, Via Ardichetto (in front of n. 22)	Carrara marble	private building
AC1	Acireale, Via Lancaster 1	Iblean calcarenite	private building
AC2	Acireale, Via dei P.P. Filippini	lime-based mortar	private building
AC3	Acireale, Vicolo dei P.P. Filippini 21	Iblean calcarenite	private building
AC4	Acireale, Vicolo Zelanti 10	Iblean calcarenite	private building
AC5	Acireale, Via Pennisi 7-9	lime-based plaster	private building
AC6	Acireale, Via Vittorio Emanuele II (in front of n. 184)	lime-based plaster	Sant'Antonio Church
AC7	Acireale, Via Vittorio Emanuele II 199-201	Iblean calcarenite	private building
AC8	Acireale, Via Vittorio Emanuele II 154	Iblean calcarenite	private building

Table 2: oxygen and sulphur multi isotopic values measured in black crusts. All values are expressed in permil ± 0.8, 0.1, 0.8, 0.01 and 0.20 (1σ) for $\delta^{18}O$, $\Delta^{17}O$, $\delta^{34}S$, $\Delta^{33}S$ and $\Delta^{36}S$ respectively. Mean values and standard deviation (2σ) for each group are indicated in bold.

Samples	**$\delta^{18}O$** SMOW	**$\Delta^{17}O$** SMOW	**$\delta^{34}S$** CDT	**$\Delta^{33}S$** CDT	**$\Delta^{36}S$** CDT
Group 1	**9.6 ± 0.8**	**0.44 ± 0.26**	**0.9 ± 1.56**	**-0.2 ± 0.09**	**-0.3 ± 0.11**
PA1	11.8	-0.07	1.36	-0.31	-0.53
PA2	11.5	0.84	0.56	-0.05	-0.37
PA3	9.3	0.52	-0.59	-0.29	-0.07
PA4	-	-	0.21	-0.4	-0.39
PA5	10.2	-0.14	-	-	-
PA6	8.6	-0.17	-0.43	-0.05	-0.38
PA7	7.2	0.02	-2.68	-0.2	-0.59
PA8	9.2	0.71	0.59	-0.18	-0.39
PA9	10.3	0.94	-	-	-
PA10	11.3	1.00	4.14	-0.1	-0.19
PA11	9.5	0.98	5.1	-0.01	-0.18
PA12	7	0.26	-	-	-
PA13	8.9	0.37	-	-	-
Group 2	**11.3 ± 1.1**	**1.61 ± 0.43**	**4.9 ± 2.52**	**-0.06 ± 0.03**	**-0.17 ± 0.11**
CT2	11.2	1.36	4.05	-0.06	-0.07
CT3	12.9	1.37	-	-	-

CT4	9.8	0.73	-	-	-
CT5	9.5	2.00	5.84	-0.08	-0.24
CT6	9	1.03	5.77	-0.1	0.41
CT7	8.9	0.97	-	-	-
CT9	16.6	3.68	-1.64	0.02	-0.2
CT10	12.7	1.78	3.99	-0.09	-0.21
CT12	10.8	0.72	2.88	-0.14	-0.36
CT14	11.9	1.24	9.13	-0.04	-0.06
CT20	13.8	2.08	1.91	-0.19	-0.43
Li1	8.5	1.27	6.51	-0.01	-0.15
Li2	13.3	1.73	10.14	0	-0.17
Li3	10.6	3.20	-0.74	-0.01	-0.19
Li4	10.1	0.44	15.04	-0.01	-0.16
Li5	11.5	2.12	0.88	-0.08	-0.33
Group 3	**13.6 ± 1.1**	**2.7 ± 0.58**	**1.6 ± 1.9**	**-0.1 ± 0.08**	**-0.2 ± 0.11**
AC1	12.9	2.81	2.62	-0.34	-0.22
AC2	12.5	1.75	5.5[illegible]	-0.02	-0.16
AC3	13.8	3.62	-1.27	-0.03	-0.44
AC4	16.2	3.01	5.[illegible]	-0.08	0.18
AC5	12	2.85	-1.74	0.01	-0.29
AC6	13	2.13	4.23	-0.05	-0.29
AC7	16.3	3.54	-0.11	-0.08	-0.2
AC8	10.4	0.47	-0.5	-0.3	-0.25
ZAF2	13.1	2.13	-	-	-
ZAF4	13	3.04	-	-	-
SV1	16.3	3.82	0.25	-0.03	-0.07

Table 3: Proportion of the different oxidation channels $f_{O2\text{-}TMI}$, f_{H2O2} and f_{O3}, that contribute to the SO_2 oxidation on the stone substrate for each group of black crust samples. The $\Delta^{17}O_{measured}$ values correspond to the average value for each group. Group1 includes black crusts from Palermo, Group 2 includes black crusts from Catania and Linguaglossa and Group 3 includes black crusts from Acireale and Zafferana. Calculation details are in supplementary material II.

Black crust	$\Delta^{17}O_{measured}$ (‰)	$f_{O2\text{-}TMI}$ (%)	f_{H2O2} (%)	f_{O3} (%)
Group 1	0.44	45-94	55-0	0-6
Group 2	1.61	0-81	91-0	9-19
Group 3	2.65	0-69	78-0	22-31

Credit author statement

E. Martin: conceptualization

E. Martin; G. Montana; L. Randazzo: collect of black crusts

A. Aroskay: oxygen and sulphur isotope measurements

AA, EM, SB, GM and contributions from all co-authors (PC, AC, AVC, LR): interpretation and writing

Declaration of interests

☒ The authors declare that they have no known competing financial interests or personal relationships that could have appeared to influence the work reported in this paper.

☐The authors declare the following financial interests/personal relationships which may be considered as potential competing interests: